Improving on Inversions for Kinematic Parameters of the Earthquake Source

Ralph J. Archuleta
University of California, Santa Barbara

Those who have helped but should not be blamed

- Pengcheng Liu
- Susana Custódio
- Morgan Page
- Chen Ji
- Steve Hartzell

The Problem

The problem remains that in many cases the fit to the data is very good even when the faulting process is poorly reproduced, so that in the real case it would be difficult to know when one has obtained the correct solution.

Das and Suhadolc, J. Geophysical Research, 1996

While extra free parameters can improve the data fit, we have shown that the data fit it not a good measure of model error, which is what modelers want to minimize.

Page, Custódio, Archuleta and Carlson, *J. Geophysical Research, 2009*

Some of the Issues with Inversions (Are We Doing the Best We Can?)

- Linearization
  - Advantages
  - Disadvantages
- Data Misfit vs Model Misfit
  - Overparameterized models
  - Constraints
- Combined Inversions
  - Two step approach
  - Weights
- Forensics
  - Looking at the model in the forward sense
- Slip rate function
- …

Inversions

- Linearized Inversions (representative sample)
  - Olson and Apsel (1982)
  - Hartzell and Heaton (1983)
  - Cohee and Beroza (1994)
  - Wald and Heaton (1994)
- Nonlinear Inversions (representative sample)
  - Cotton and Campillo (1994, 1995)
  - Hartzell and Liu (1995)
  - Ji, Wald and Helmberger(2002)
  - Liu and Archuleta (2004)
  - Emolo and Zollo (2005)
  - Piatenesi, Cirella, Spudich and Cocco (2007)
  - Hartzell, Liu, Mendoza, Ji and Larson (2008)

Kinematic Model (Haskell, 1964)

- ***Fault Geometry: Length, Width***
- ***Slip***
- ***Rise Time***
- ***Rupture Velocity***

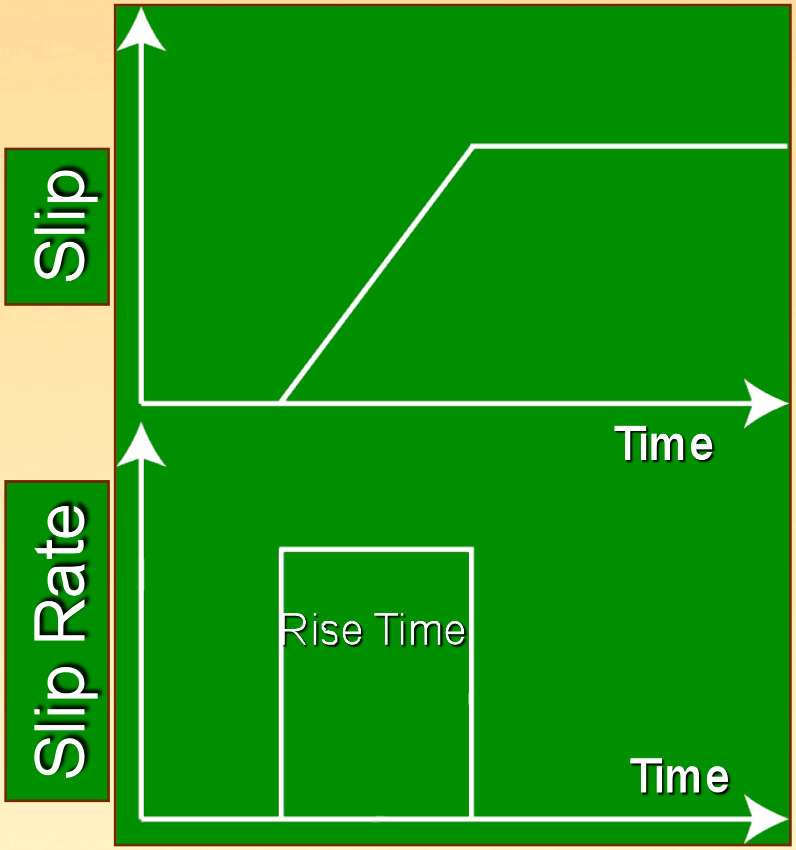

Inversion Parameters

Slip rate time function

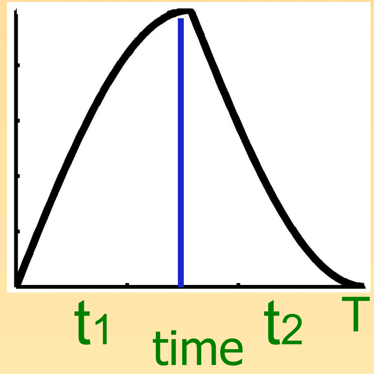

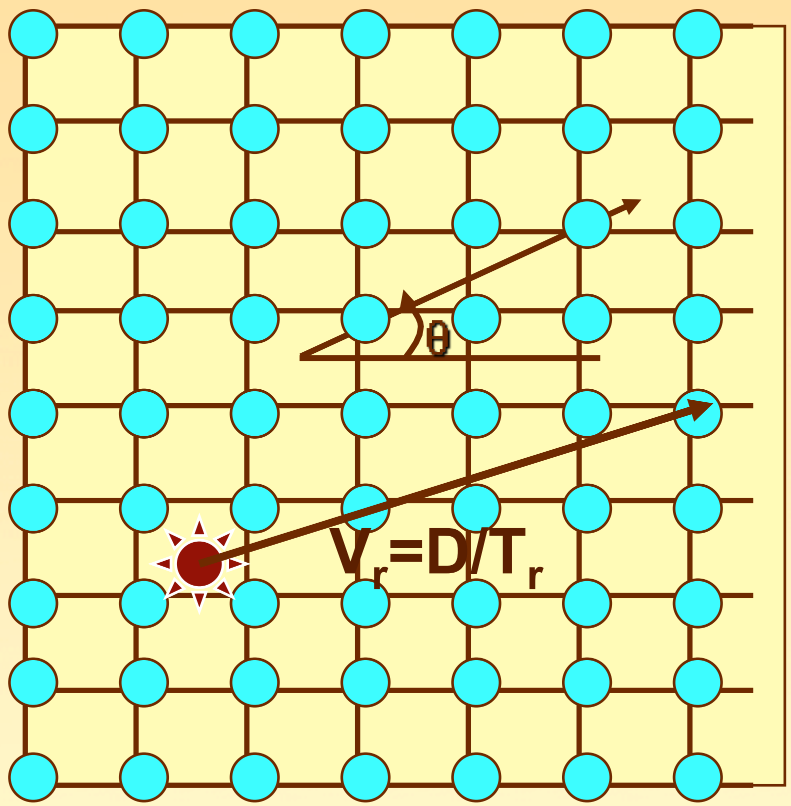

Source parameters:

- Slip amplitude (**A**)
- Slip rake (θ)
- Rupture velocity
- Rise time (**t_1, t_2**)

Liu and Archuleta, JGR, 2004

Linearization

Basic Problem: Time variables are not linearly related to the data.

- Approximate the problem by allowing multiple time windows for each point on the fault.
- Slip rate function for each window is specified, e.g., triangles
- Rupture velocity is nearly constant; most times the rupture velocity is fixed.
- Excellent study done by Brian Cohee and Greg Beroza, Annali di Geofisica, Vol 37, Dec. 1994.

Linearization

Brian Cohee and Greg Beroza, *Annali di Geofisica*, Vol 37, Dec. 1994.

- Single window overestimates seismic moment by 20% while multi-window overestimates by ~60% also noted by Hartzell (1989).
- Single window recovers the average rupture velocity and basic location of the slip; three window inversion fit more of the noise in the data and consequently added erroneous moment to the model. The variance reduction with multiple windows is only marginally better than a single window.
- If the slip distribution is known in advance, e.g., through GPS data, the rupture velocity variation is more reliably imaged.

Representation Theorem

$$u_n(\boldsymbol{x},t) = \int_{-\infty}^{\infty} d\tau \iint_{\Sigma} \left[u_i(\xi,\tau) \right] c_{ijpq} \nu_j \partial G_{np}(\boldsymbol{x},t-\tau;\xi,0) / \partial \xi_q \; d\Sigma$$

Aki and Richards, (3.2)

$$\hat{\mathbf{a}} \bullet \ddot{\mathbf{u}}^s = \ddot{f}_r * \int_{\mathbf{y}(t,\mathbf{x})} \left[c^2 \left(\frac{d\mathbf{s}_r}{dq} \bullet \mathbf{G}_a^s \right) + c^2 \left(\frac{d\mathbf{G}_a^s}{dq} \bullet \mathbf{s}_r \right) + \frac{dc}{dt} \left(\mathbf{s}_r \bullet \mathbf{G}_a^s \right) \right] dl$$

Slip Rate Time Function

Stress Drop (spatial derivative of slip)

Change in isochrone Velocity ~ acceleration of the the rupture front

Spudich and Frazer, BSSA, 1984

Object Function

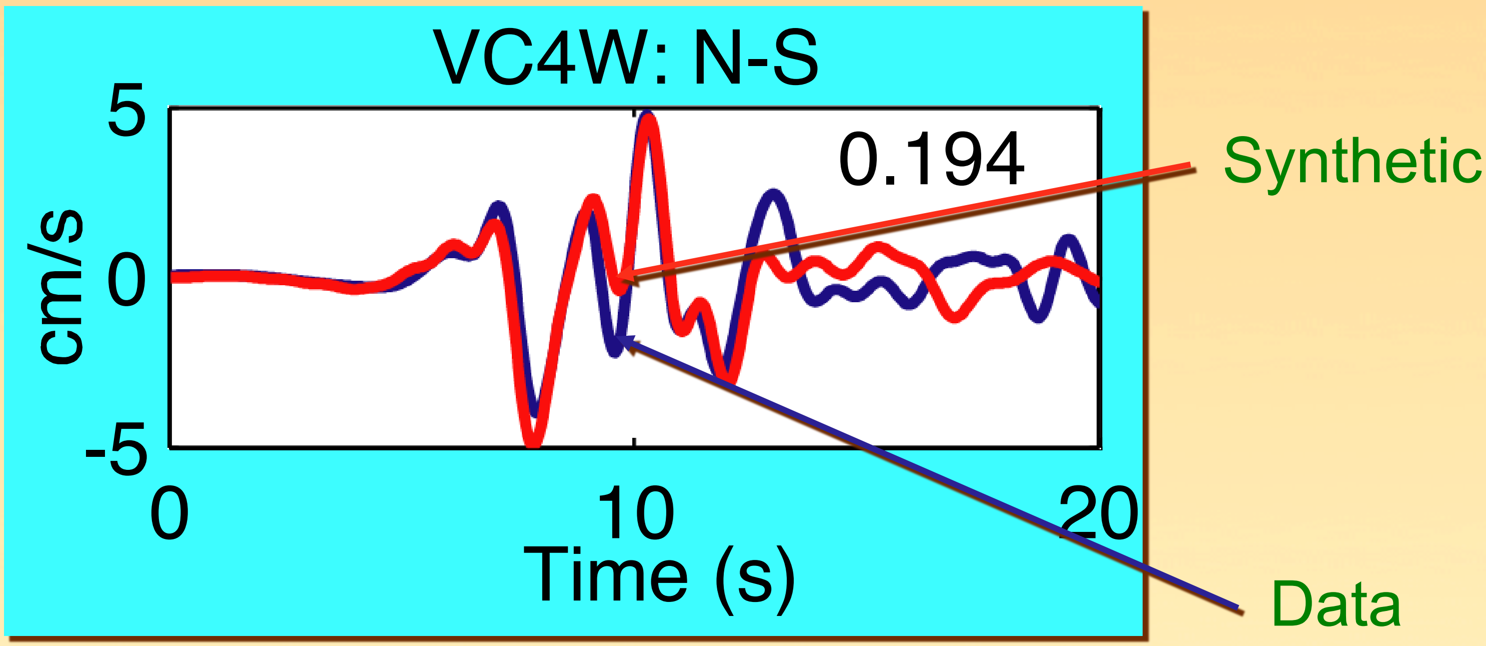

$$m(Model) = \sum_{1}^{N_d} W_d \left(1 - \frac{2\sum_{t_b}^{t_e} (u_{dat}(t)\, u_{syn}(t))}{\sum_{t_b}^{t_e} u_{dat}^2(t) + \sum_{t_i}^{t_f} u_{syn}^2(t)} \right) + W_c(constraints)$$

Misfit — (data – synthetics) — constraints

Spudich and Miller, BSSA, 1991
Liu and Archuleta, JGR, 2004

Data Misfit

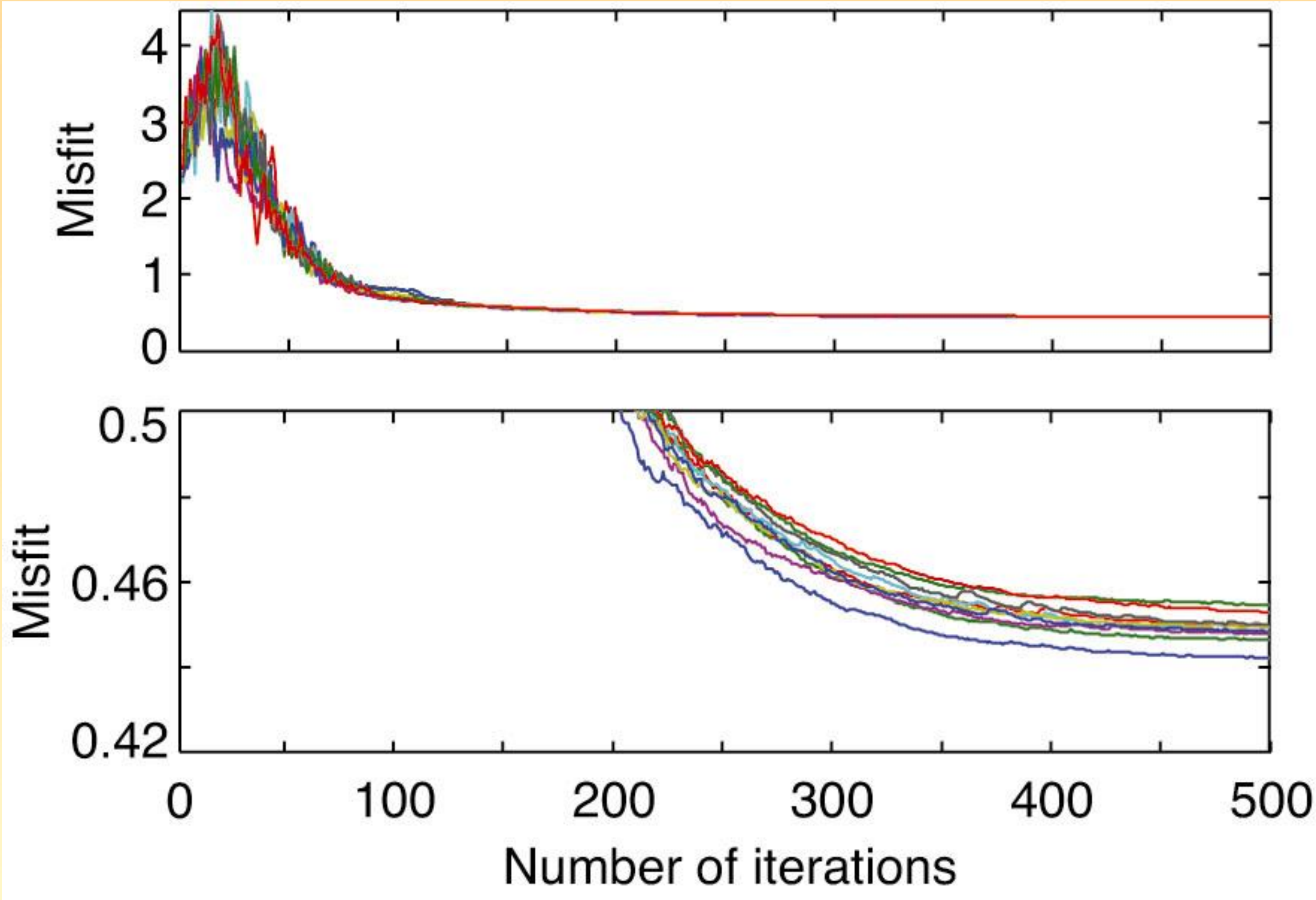

4
3
2
1
0
Misfit
0.5
0.46
0.42
Misfit
0
100
200
300
400
500
Number of iterations

Waveforms (inverted): Fault Normal

Misfit of inversion: m_{inv}=0.31

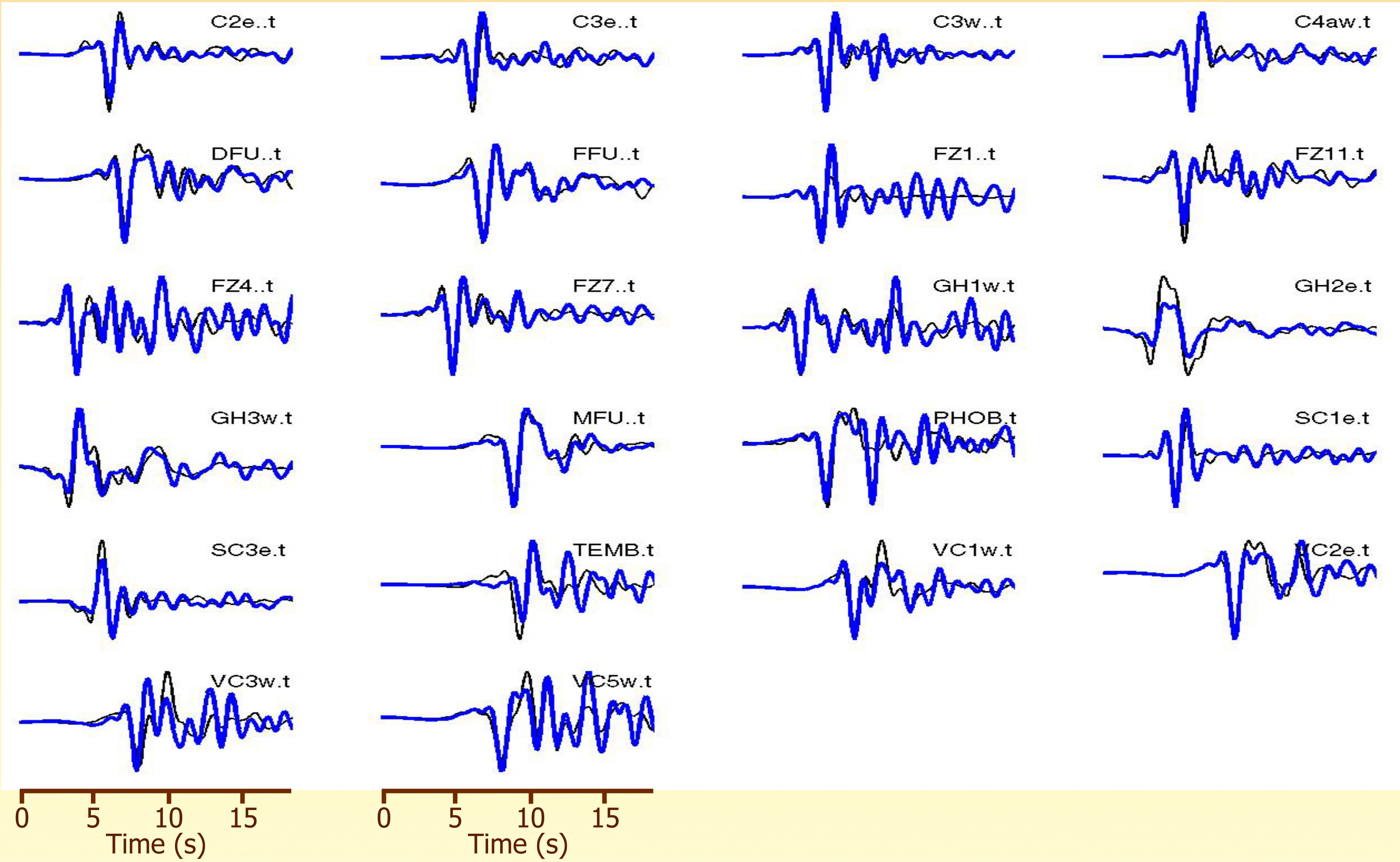

Custódio, Liu and Archuleta, GRL, 2005

Waveforms (predicted): Fault Normal

Misfit of inversion: m_{pred}=0.63

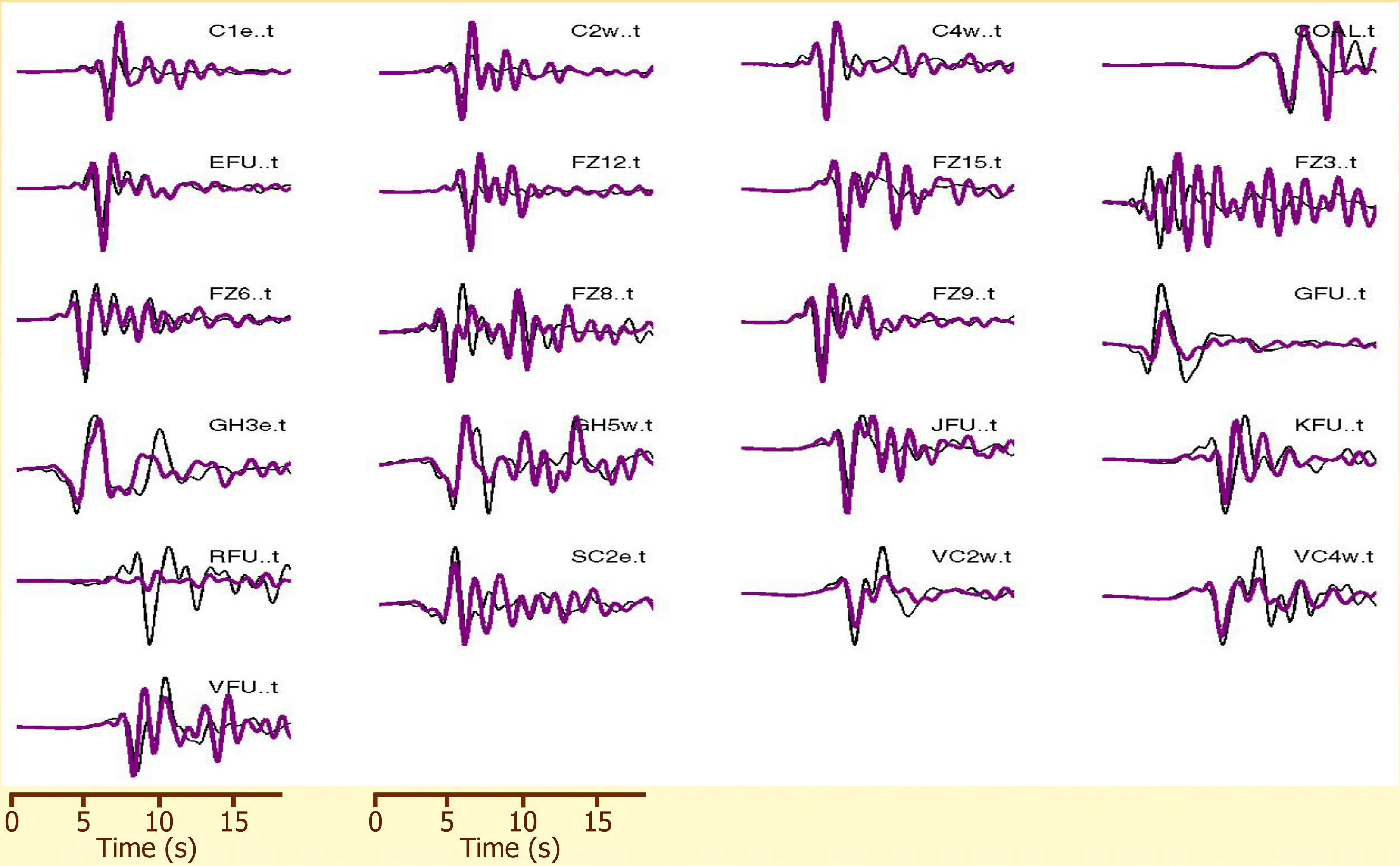

Custódio, Liu and Archuleta, GRL, 2005

Parkfield Data

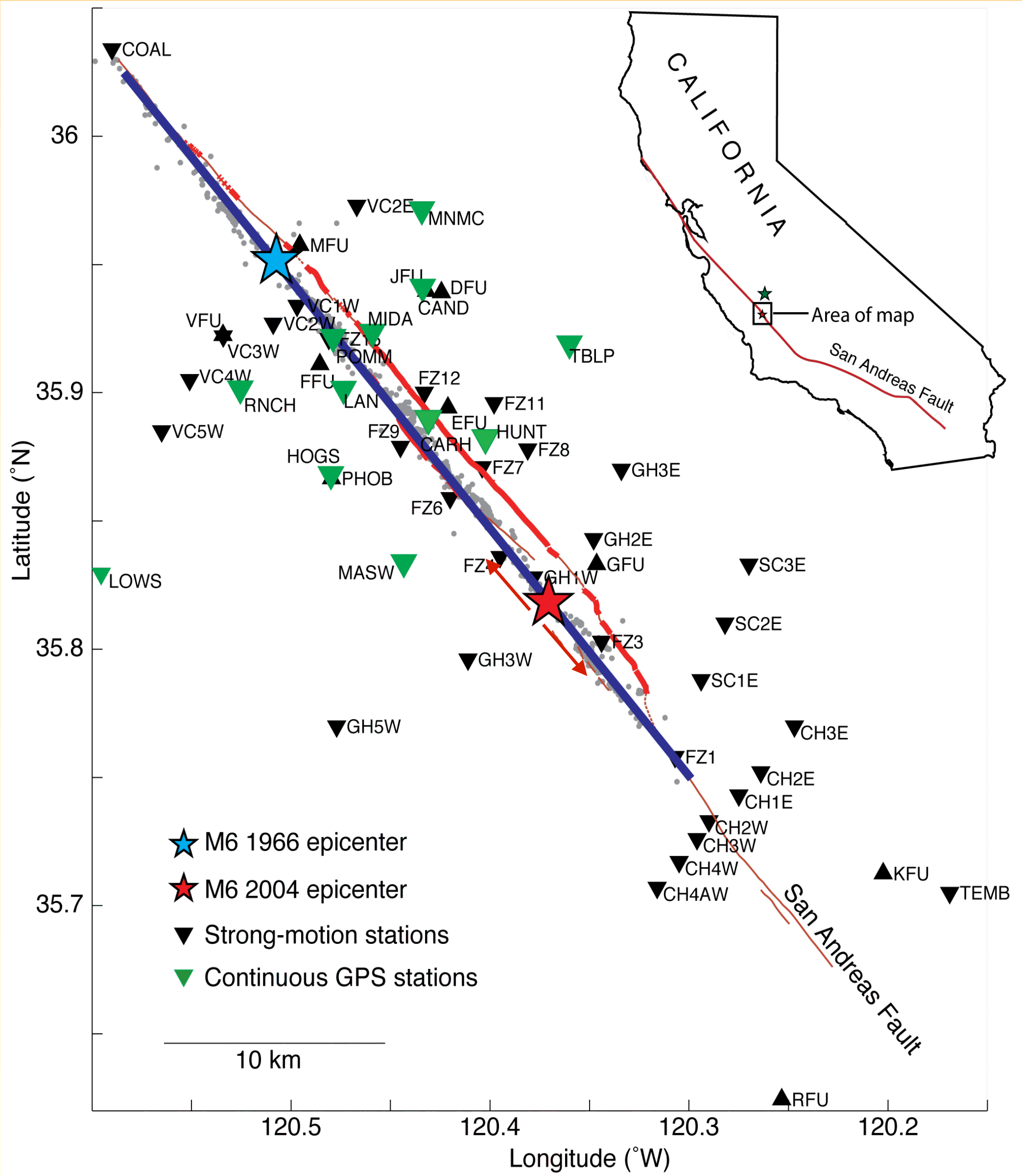

Model Misfit: Average of 12 Sets of Data

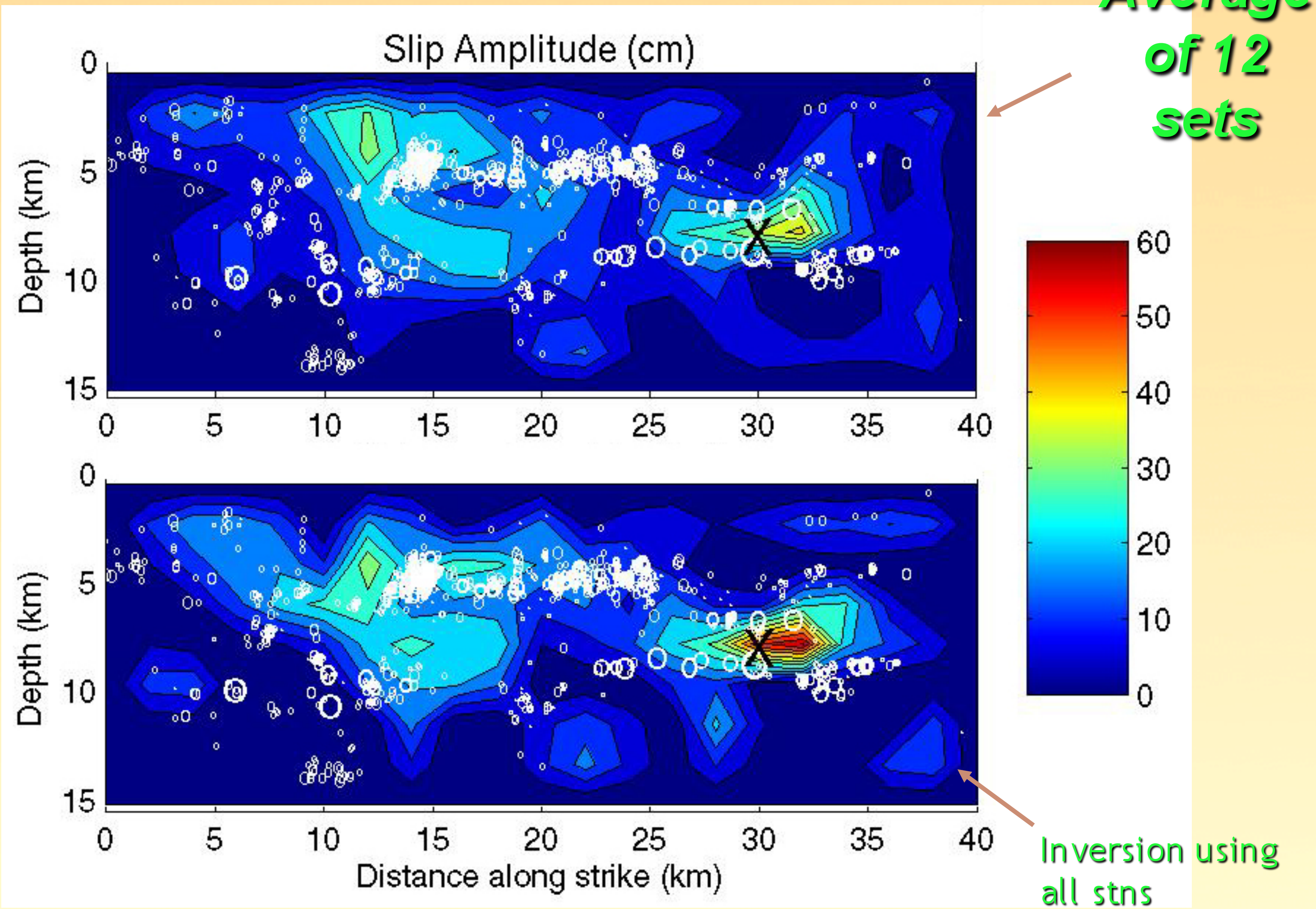

Custódio, Liu and Archuleta, GRL, 2005

Model Uncertainty

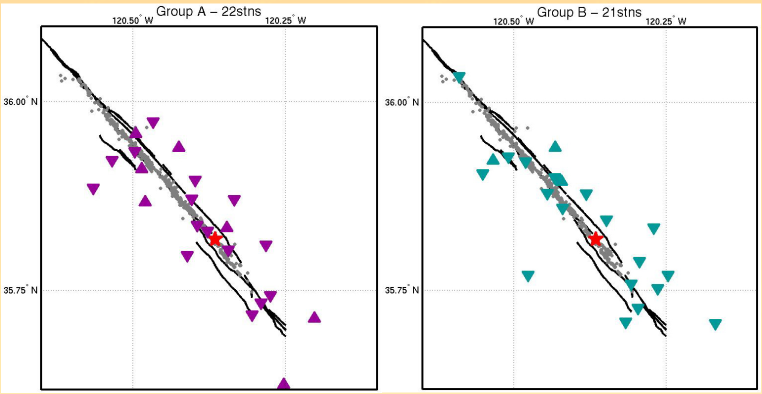

Average of 12 models computed based on different subsets of data

Minimum Misfit Model

Average

Standard Deviation

Coefficient of Variation

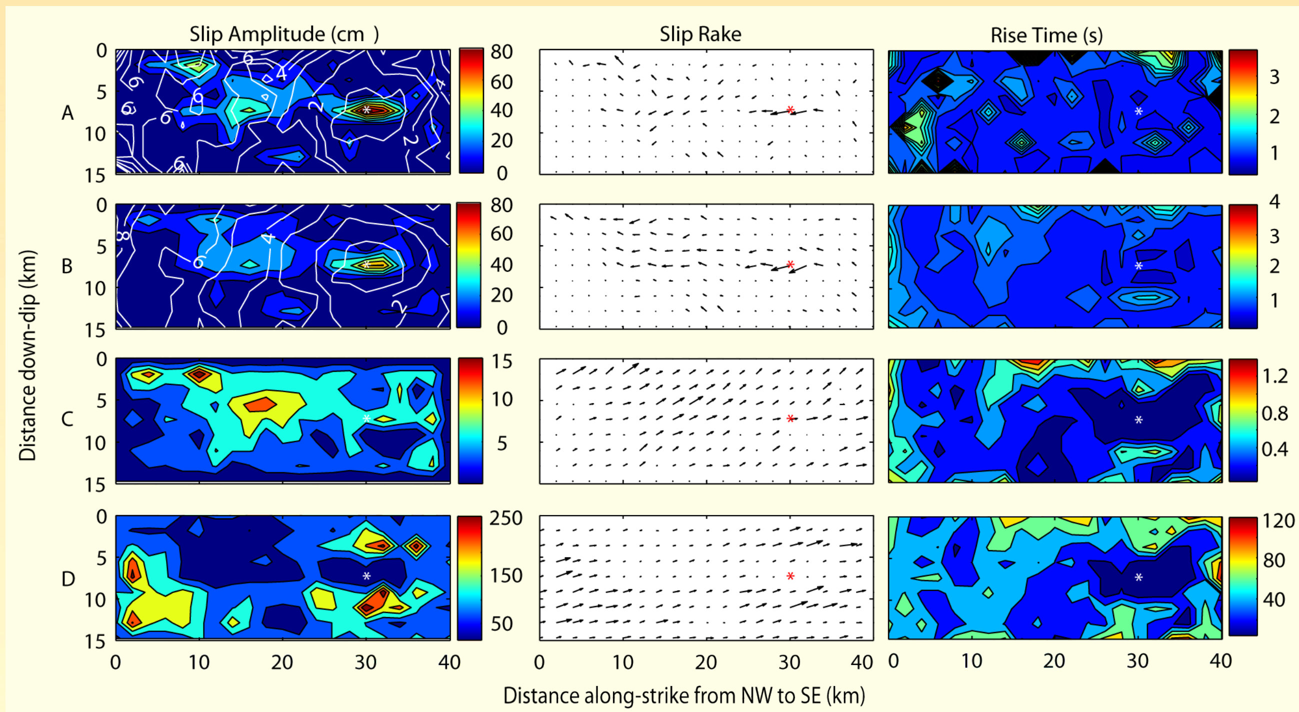

Custódio, Liu, Archuleta, GRL 2005

Model Uncertainty?

Average of 10 equally good models

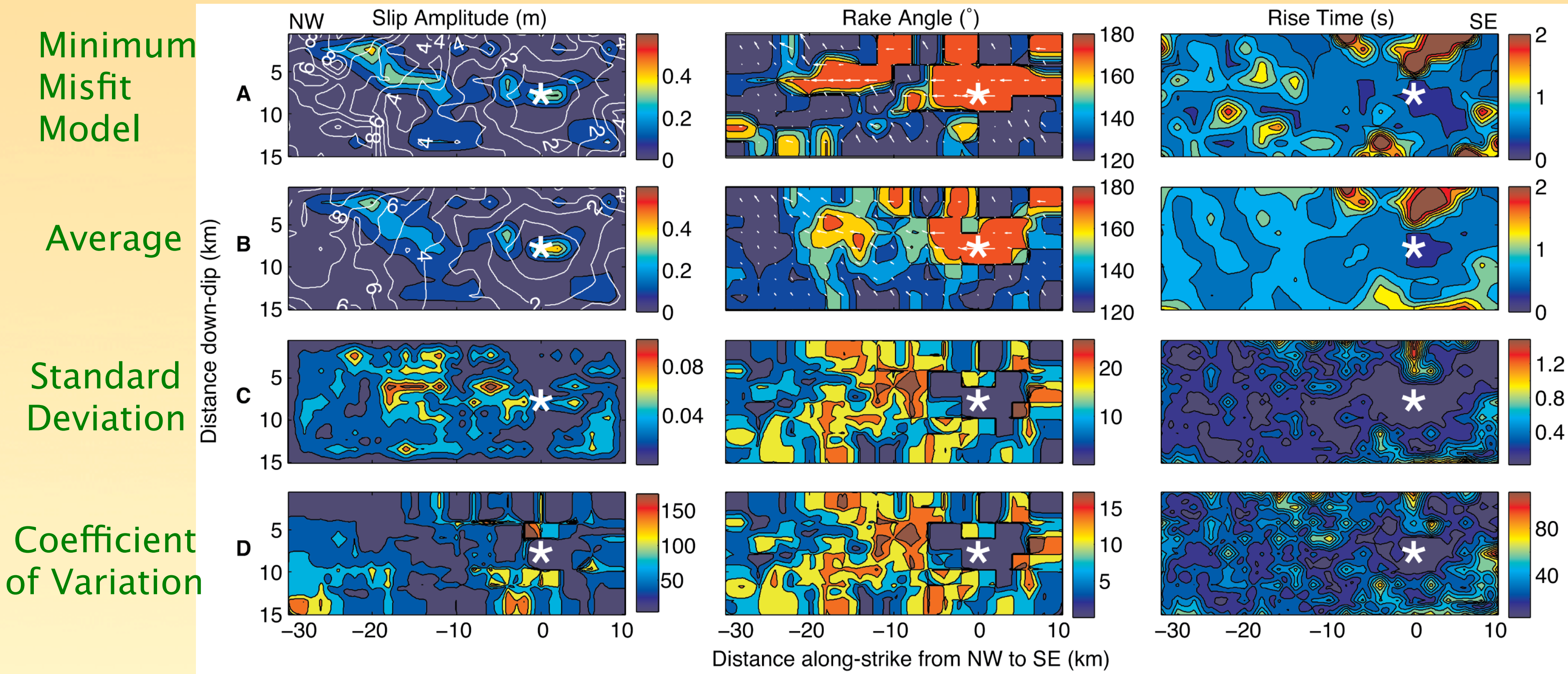

SCEC 2009 Annual Meeting Workshop

Liu, Custódio, Archuleta, BSSA 2006

Teleseismic Data: Imperial Valley

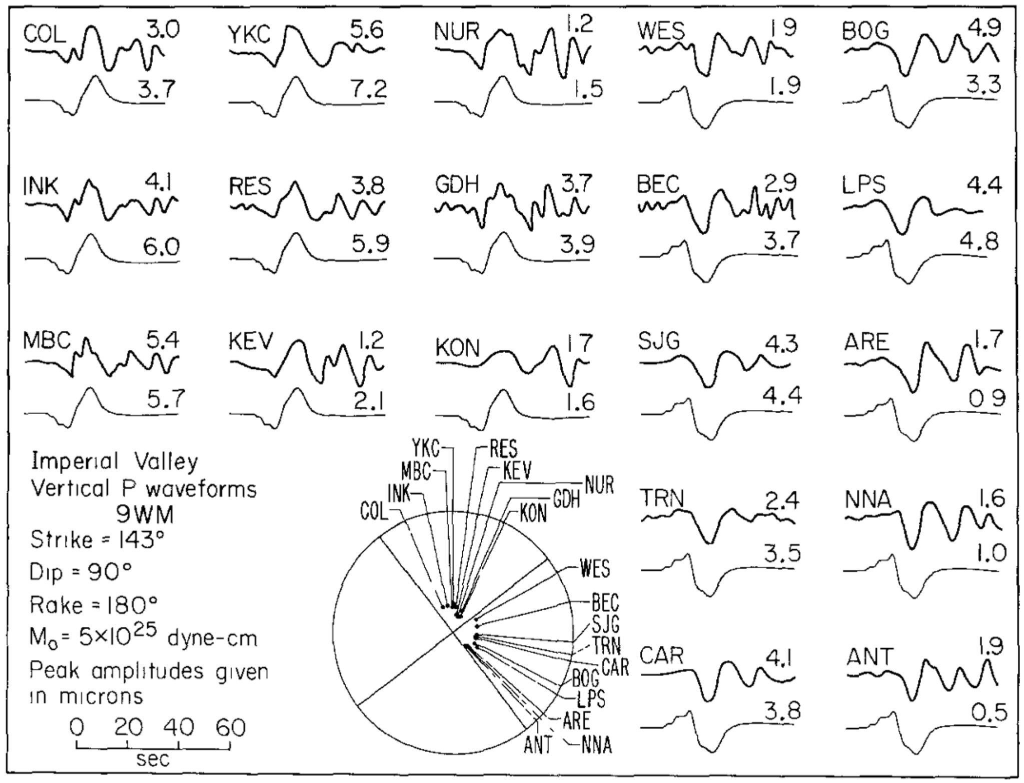

FIG 2. Comparison of observed (*top trace*) and computed (*bottom trace*) teleseismic, long-period, vertical *P* waves for model 9WM of Hartzell and Helmberger (1982). Amplitudes of synthetics are for a moment of 5.0×10^{25} dyne-cm.

Hartzell & Heaton, 1982

Seismic Data: Loma Prieta

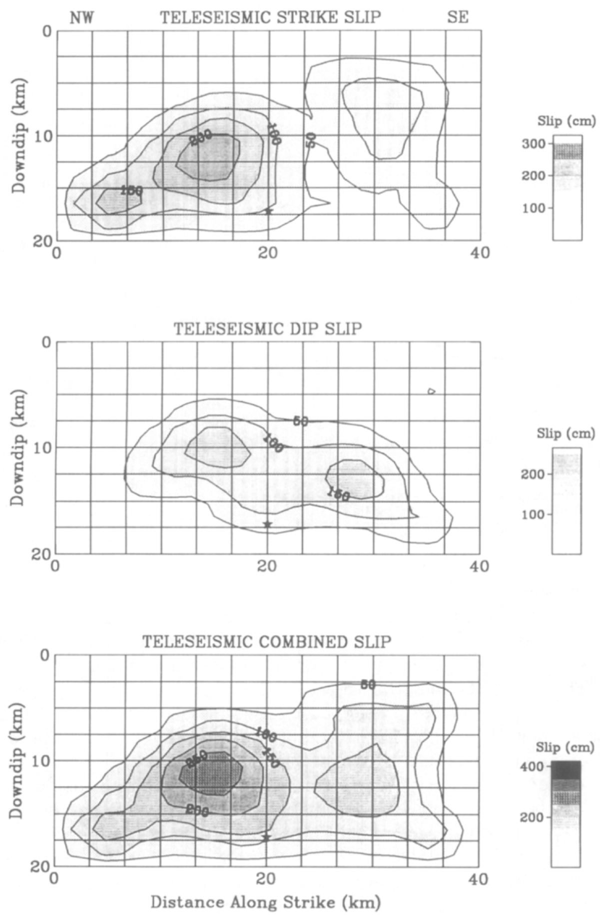

FIG. 5. Northwest-southeast cross section of the fault model showing contours of dislocation for strike-slip (*top*), dip-slip (*middle*), and oblique-slip (*bottom*) resulting from the teleseismic inversion. Contour interval is 50 cm. Shading values indicating slip in cm are given by the scale to the right of each diagram.

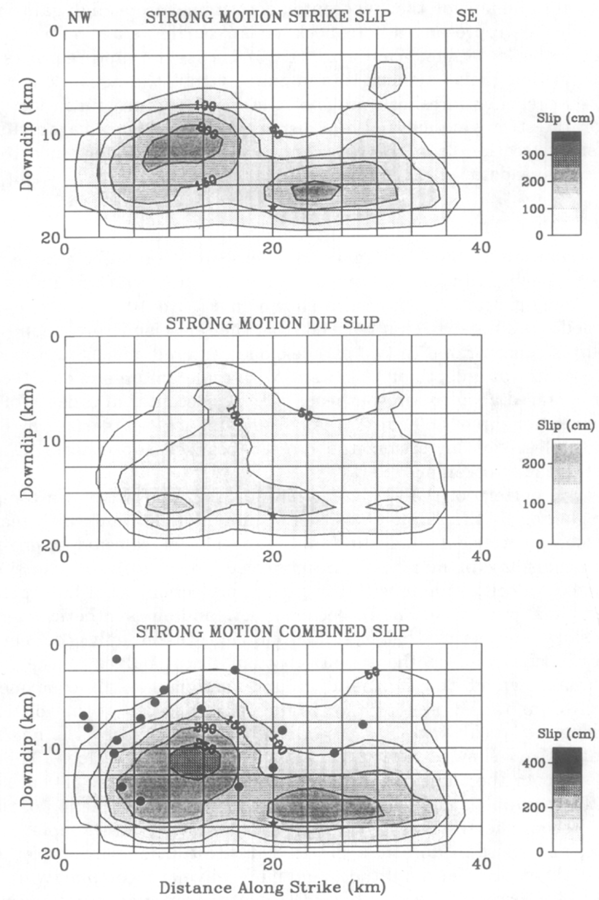

FIG. 9. Northwest-southeast cross section of the fault model showing contours of dislocation for strike-slip (*top*), dip-slip (*middle*), and oblique-slip (*bottom*) resulting from the strong-motion inversion. Contour interval is 50 cm. Shading values indicating slip in cm are given by the scale to the right of each diagram. Aftershocks with $M > 4.0$ projected onto the fault plane are represented as solid circles.

Wald, Heaton and Helmberger, BSSA 1991

Different Data Sets: Northridge

D. J. Wald, T. H. Heaton, and K. W. Hudnut

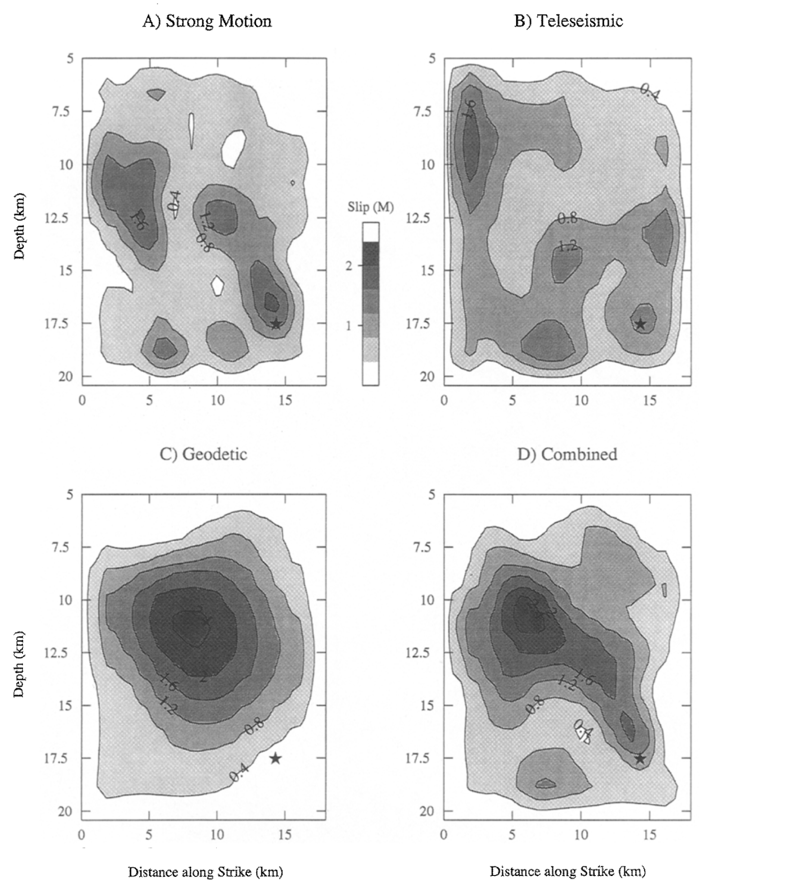

Figure 4. Comparison of the cross sections of the (a) strong-motion, (b) teleseismic, (c) geodetic, and (d) combined dislocation models. Contour interval is 0.4 m. View is from the southwest and perpendicular to (above) the fault plane. The scale bar shows the slip shading in 0.4-m increments.

Wald, Heaton & Hudnut BSSA 1996

Combined Inversion: Hector Mine

Separate Inversion

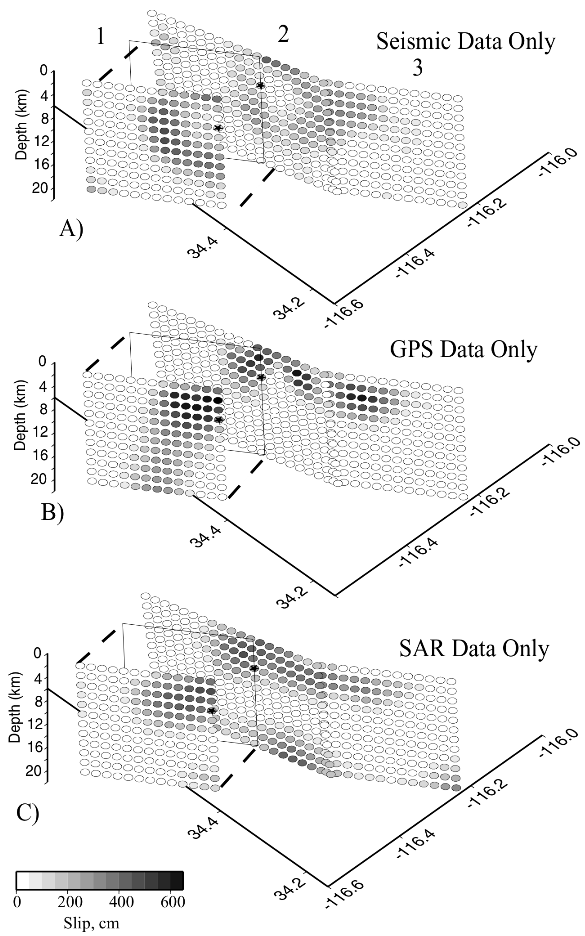

Figure 2. Slip distribution obtained by separate inversions of (A) seismic, (B) GPS, and (C) SAR data. Hypocenter is marked with a star. The gray scale shows the range in slip in centimeters. The size of the symbols represent the subfault dimension of 2 km.

Combined Inversion

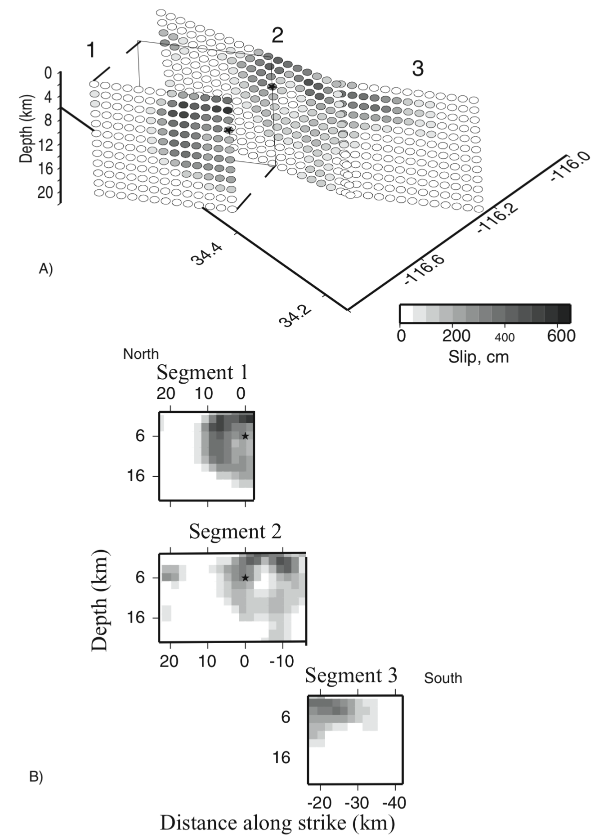

Figure 6. Preferred inversion results for the combined inversion. The hypocenter is marked with a star. The individual subfault slip is shown according to the grayscale bar. (A) 3-D representation of the slip model. The bold numbers refer to the fault segments discussed in the text. (B) A 2-D representation of the slip model.

Kaverina, Dreger and Price, BSSA, 2002

Weighting

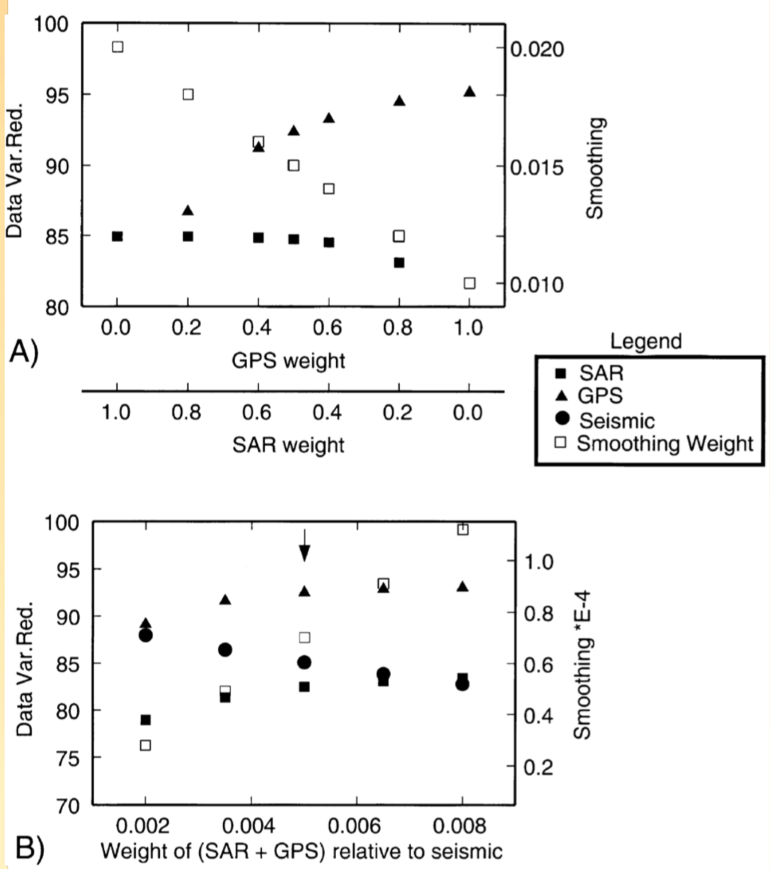

Figure 4. (A) Trade-off curves of relative GPS to SAR weighting and smoothing weight for a simultaneous inversion of geodetic data. (B) Trade-off curves for the combined seismic geodetic data inversions. The arrow indicates the preferred weighting. Variance reduction is given on the left axis and smoothing weight on the right axis. The legend for both plots is shown on the right.

GPS and SAR ~ 0.4 and 0.6, respectively

Seismic ~ 0.003

Kaverina, Dreger and Price, BSSA, 2002

1D vs 3D Green's Functions

1D

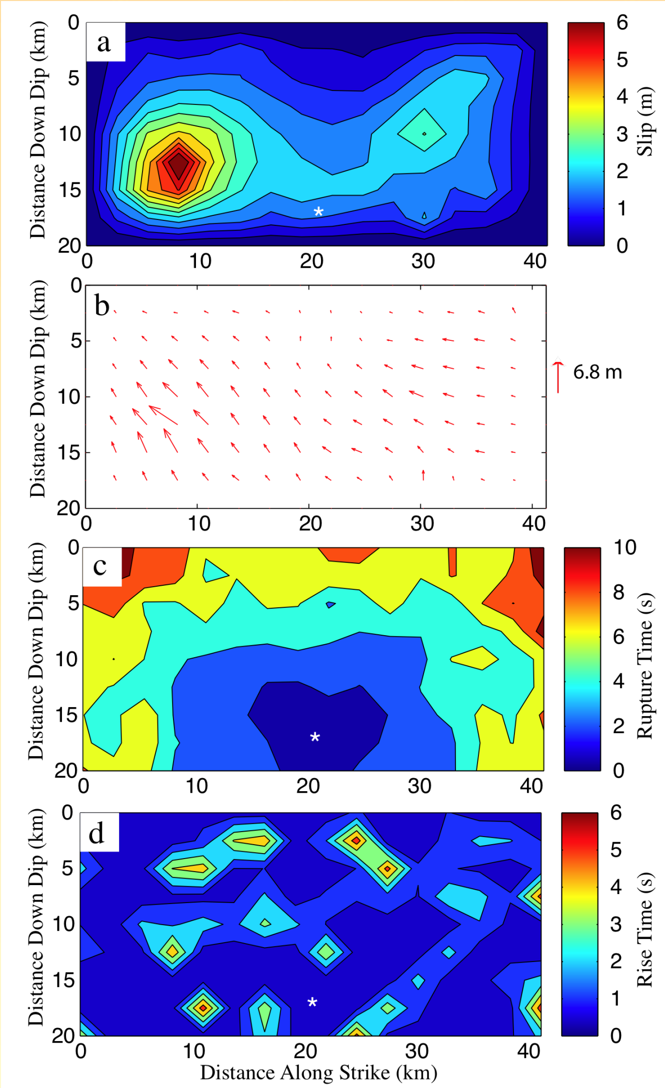

3D

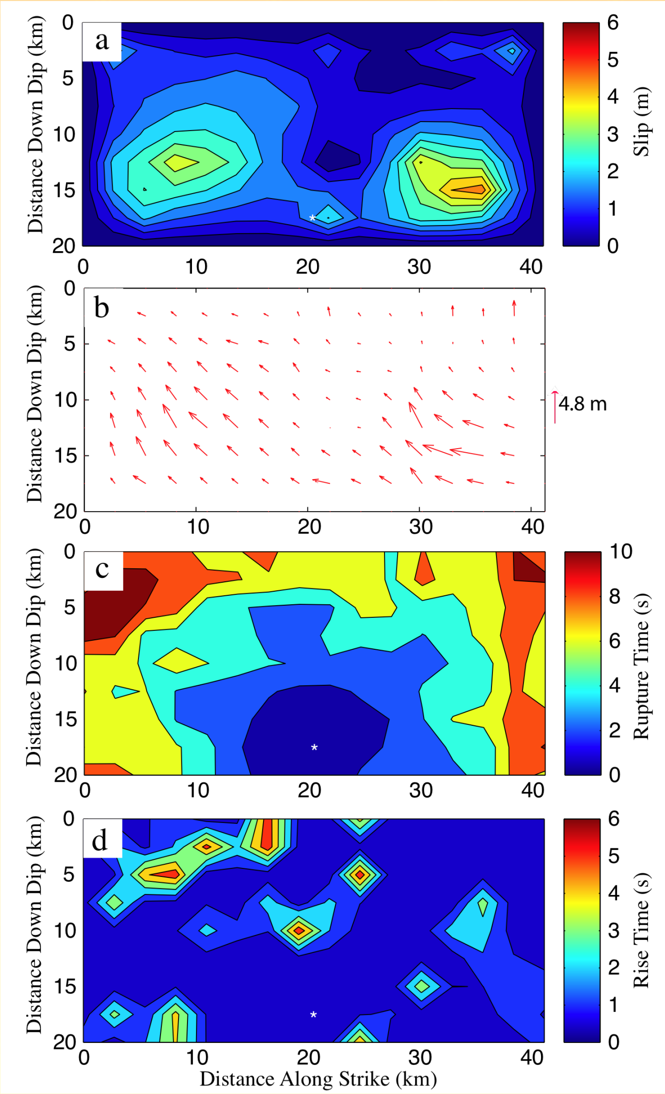

Liu and Archuleta, JGR, 2004

Two-Step Combined Seismic and GPS: 1st Step – Inversion of GPS Data Linearly Related to Slip

Input

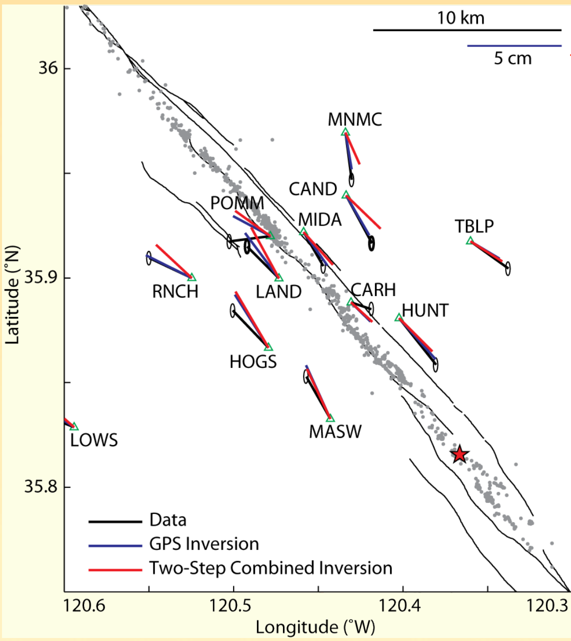

Inversion

Non-Negative Least Squares Algorithm

(Lawson and Hanson, 1974)

Output

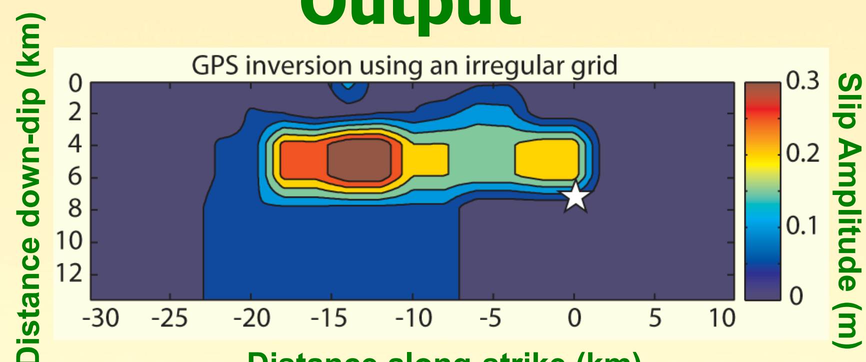

Two-Step Combined Seismic and GPS: 1st Step – Inversion of GPS Data

Resolution of Parkfield continuous GPS network

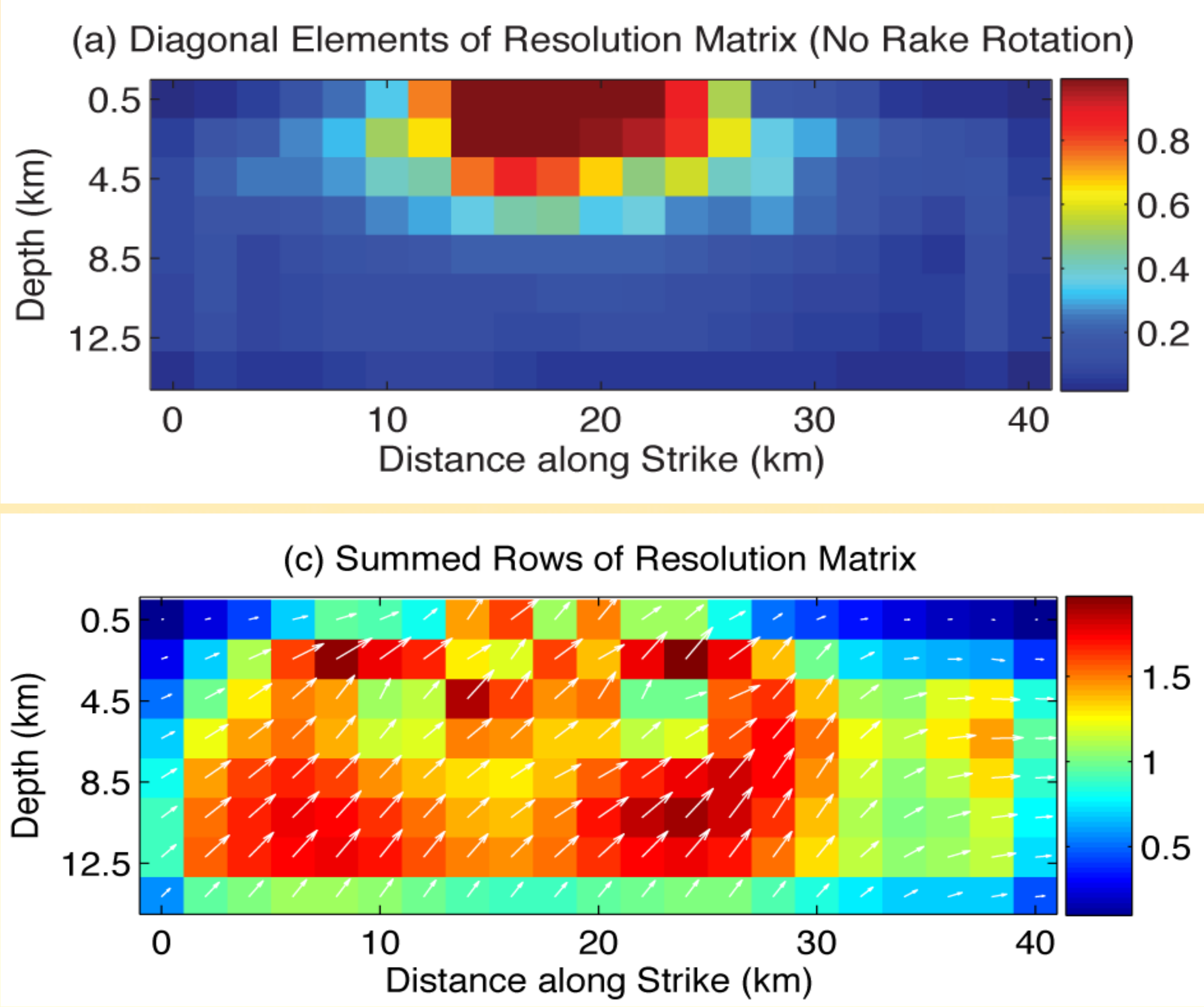

Page et al. JGR, 2009

Two-Step Combined Seismic and GPS

GPS

Seismic

Combined GPS and Seismic

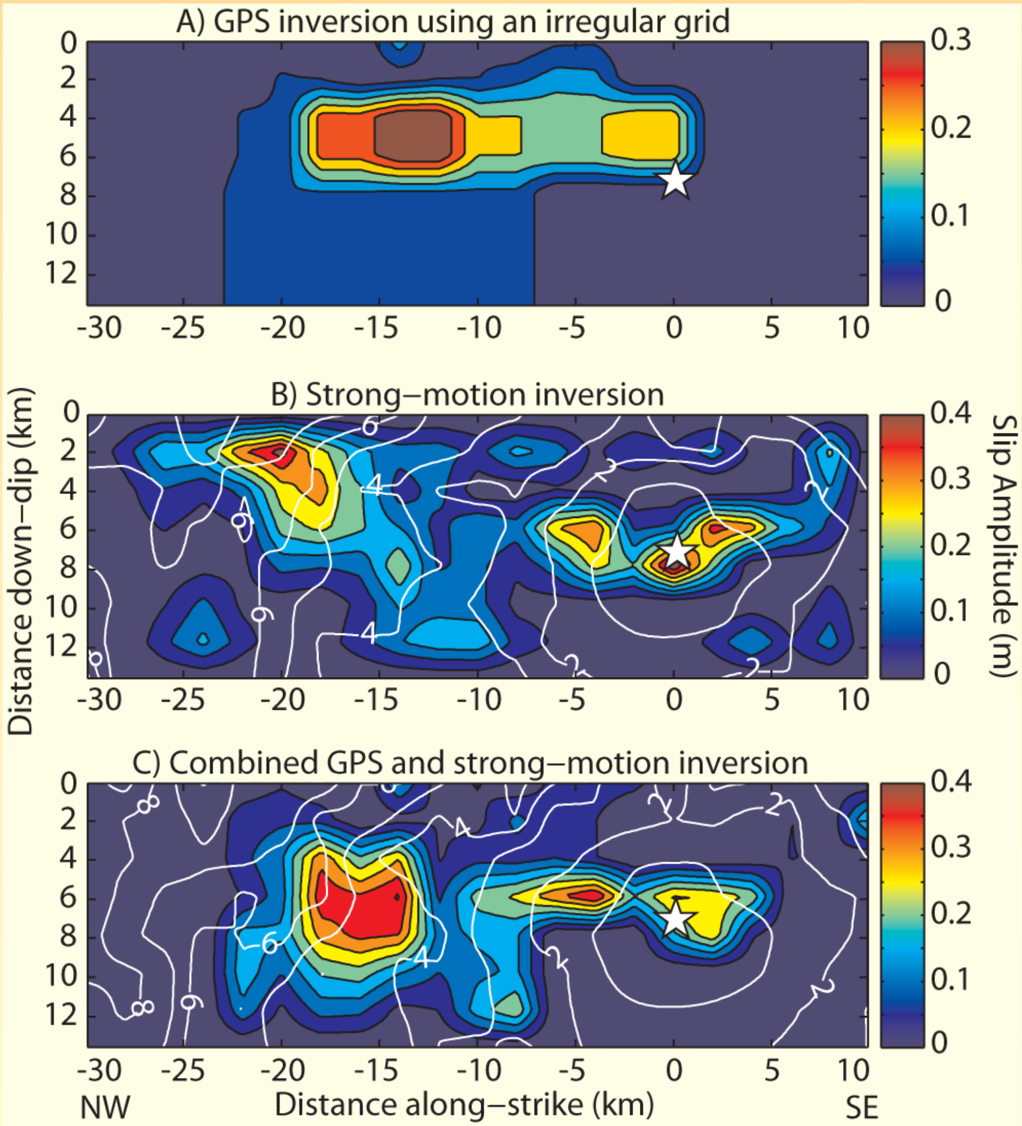

Custódio et al., JGR 2009

Slip Distributions of Four Slip Models
Blind Test

Target Model

Model I

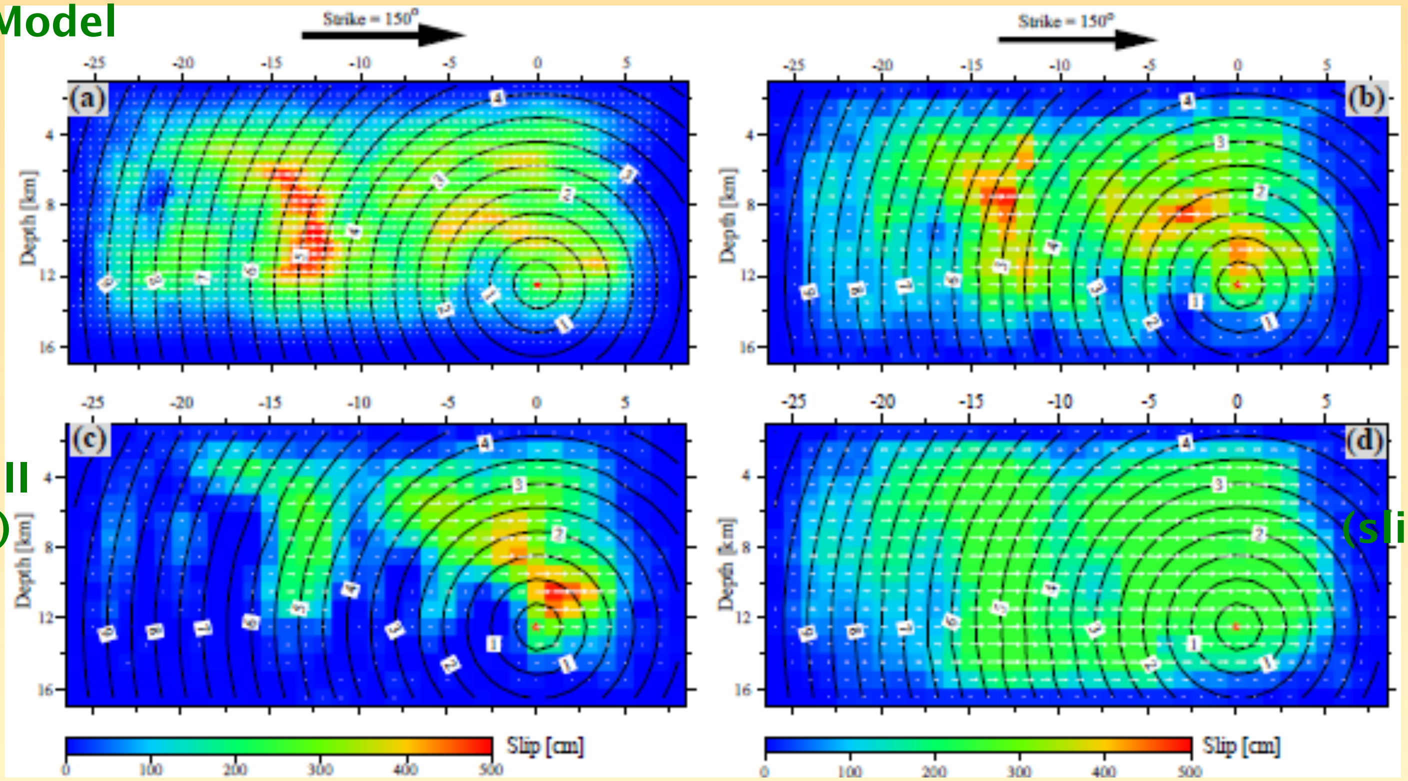

Model II
(0.5*Mo)

Model III
(slip<250 cm

Only the slip and rise time function have been inverted.

Shao and Ji, 2009

Comparison of Moment Rate Functions

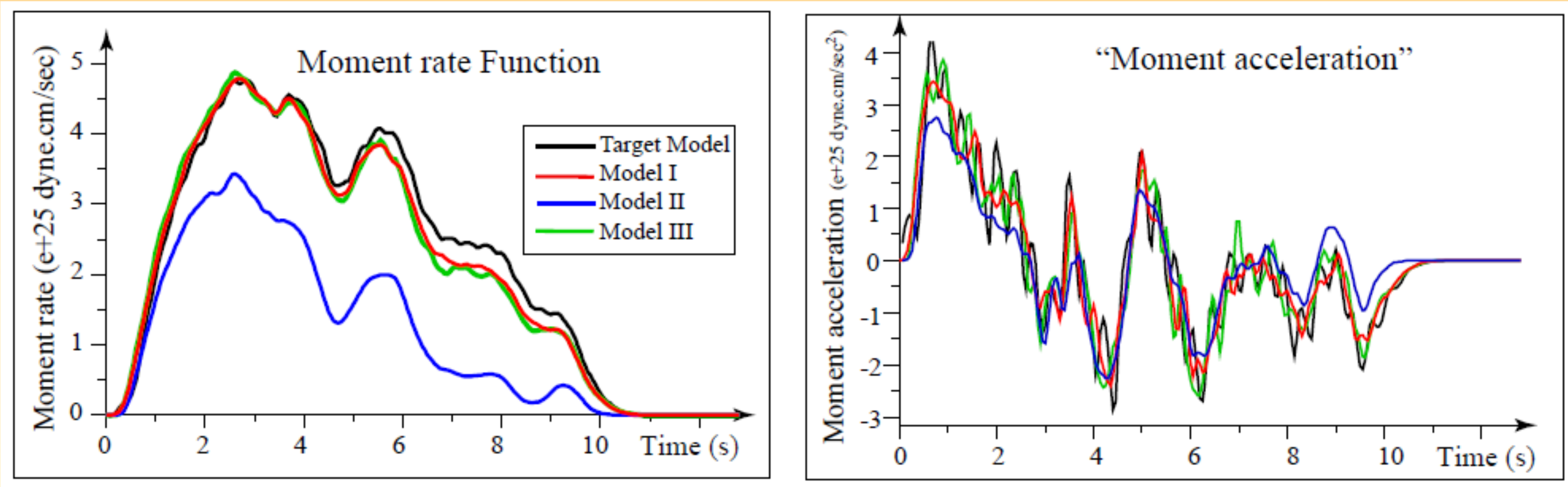

Far field body-wave

Displacement $$U(\vec{x},t) \approx \frac{1}{4\pi\rho v^3}\psi(\theta,\phi)\frac{1}{r}\dot{M}(t-r/v)$$

Velocity $$V(\vec{x},t) \approx \frac{1}{4\pi\rho v^3}\psi(\theta,\phi)\frac{1}{r}\ddot{M}(t-r/v)$$

Shao and Ji, 2009

Final Thoughts

- Must use models to predict data not used in the inversion.
- Few have addressed uncertainty in Green's functions.
- Rise time remains almost un-resolvable.

Thanks


WELL, I SUPPOSE THINGS DON'T GET WORSE THAN HANGING FROM A HELIUM BALLOON A MILE ABOVE SOME UNRECOGNIZED STATE.
OF COURSE, MY GRIP COULD WEAKEN, OR I COULD GET SUCKED INTO A JET INTAKE.
THAT'S ONE OF THE REMARKABLE THINGS ABOUT LIFE. IT'S NEVER SO BAD THAT IT CAN'T GET WORSE.
WATTERSON
7-8


HMT
Th-Th- That's All Folks

Two-Step Combined Seismic and GPS: 1st Step – Inversion of GPS Data

Regular vs Irregular Grid

- **A regular grid fails to capture the true slip**

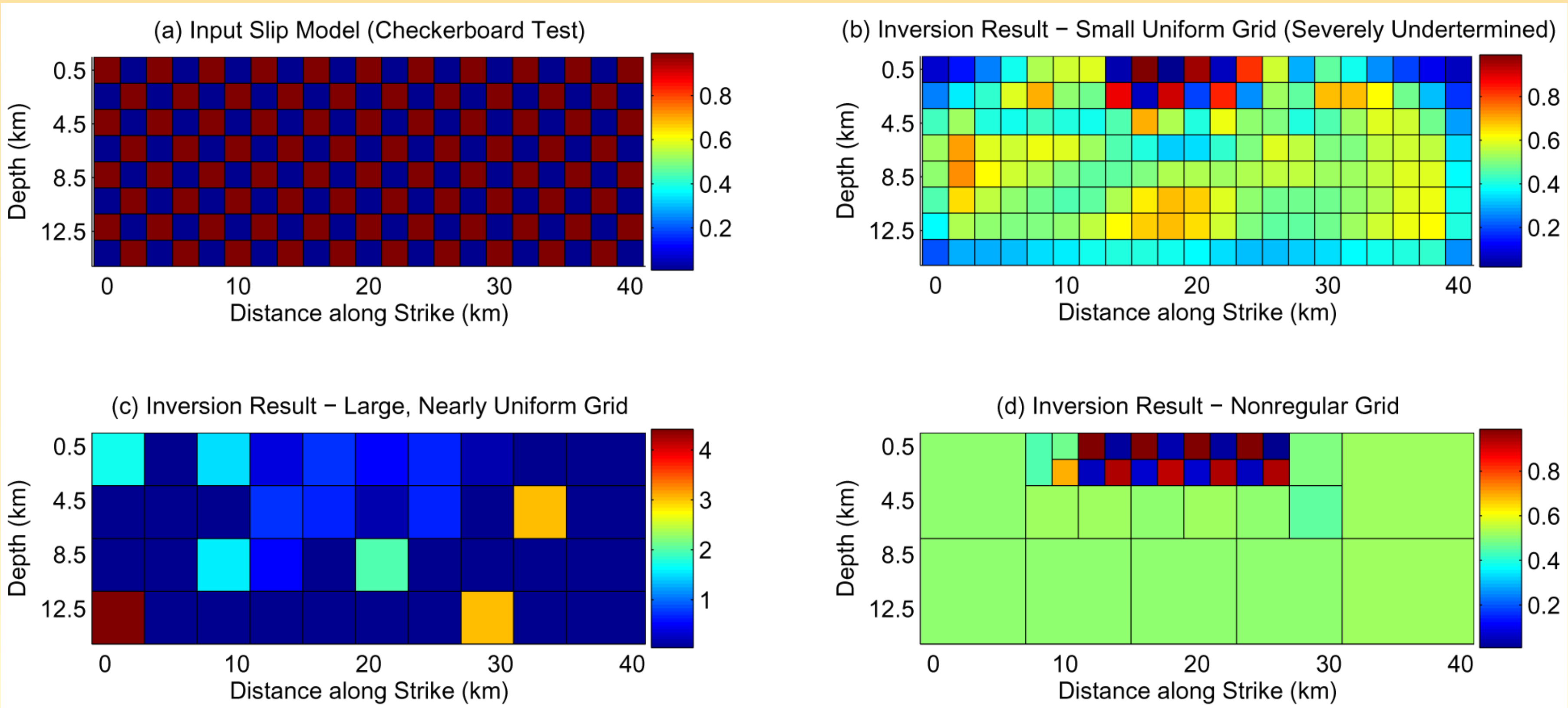

See Poster S51-0499, M. Page et al.

Page et al. (JGR submitted)

Kinematics of the 2004 Parkfield Earthquake

- **Slip amplitude:**
  - **Two clearly separate patches of slip:**
    1. **Hypocenter.**
    2. **Beneath Middle Mountain.**
- **Rupture velocity:**
  - **Very fast at hypocenter.**
  - **Then slows down to sub-shear values.**
- **Rise time:**
  - **Short, under 1 second (not well resolved).**

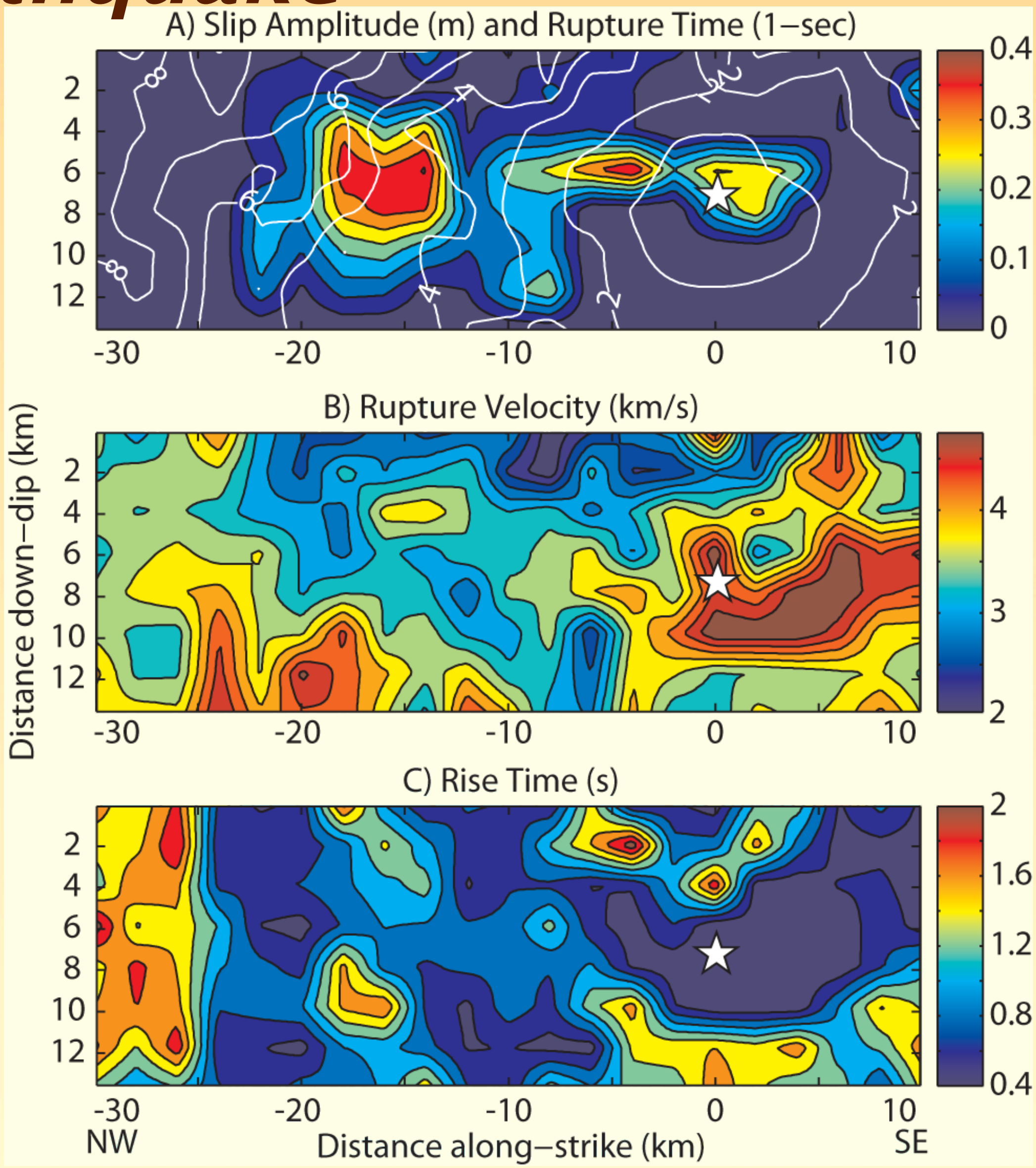

Custódio et al. (JGR submitted)

Kinematic Inversion: Seismic and GPS Data

- GPS:
  - records displacements
  - records the static field
  - captures the slip amplitude
  - resolution decays as 1/ r^2

- Seismic:
  - records accelerations
  - records the dynamic wavefield
  - captures the full temporal evolution of slip
  - resolution decays as 1/r

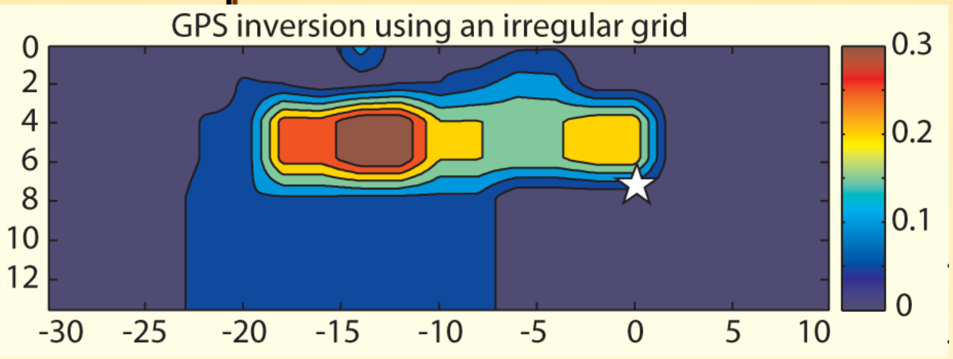

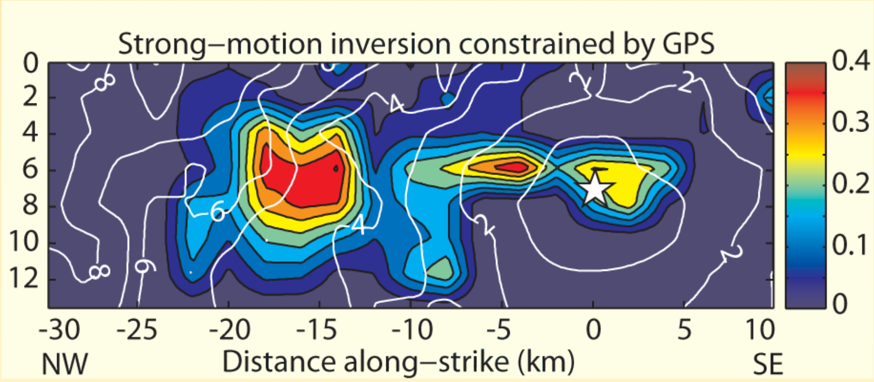

Custódio et al. (JGR submitted)

Two-Step Combined Seismic and GPS: 2nd Step – Inversion of Seismic Data

Input

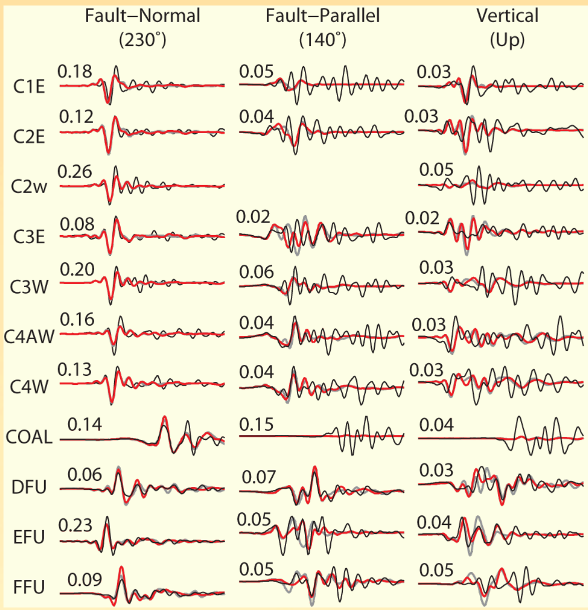

\+

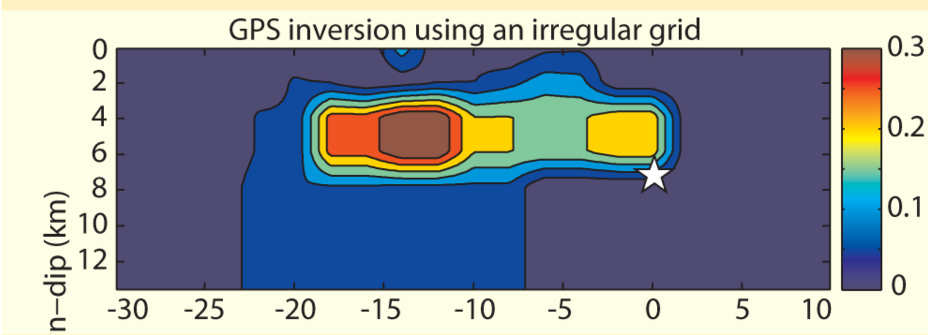

Inversion

Nonlinear

Liu and Archuleta

Output

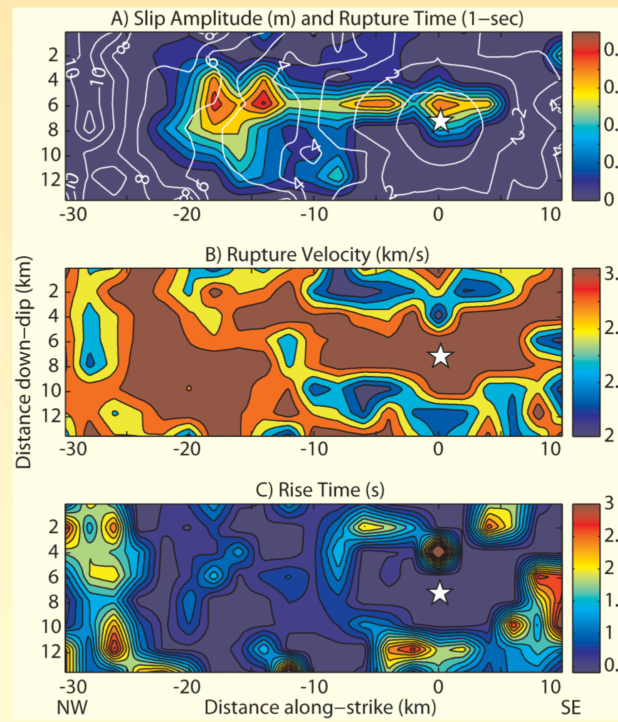

Inversion

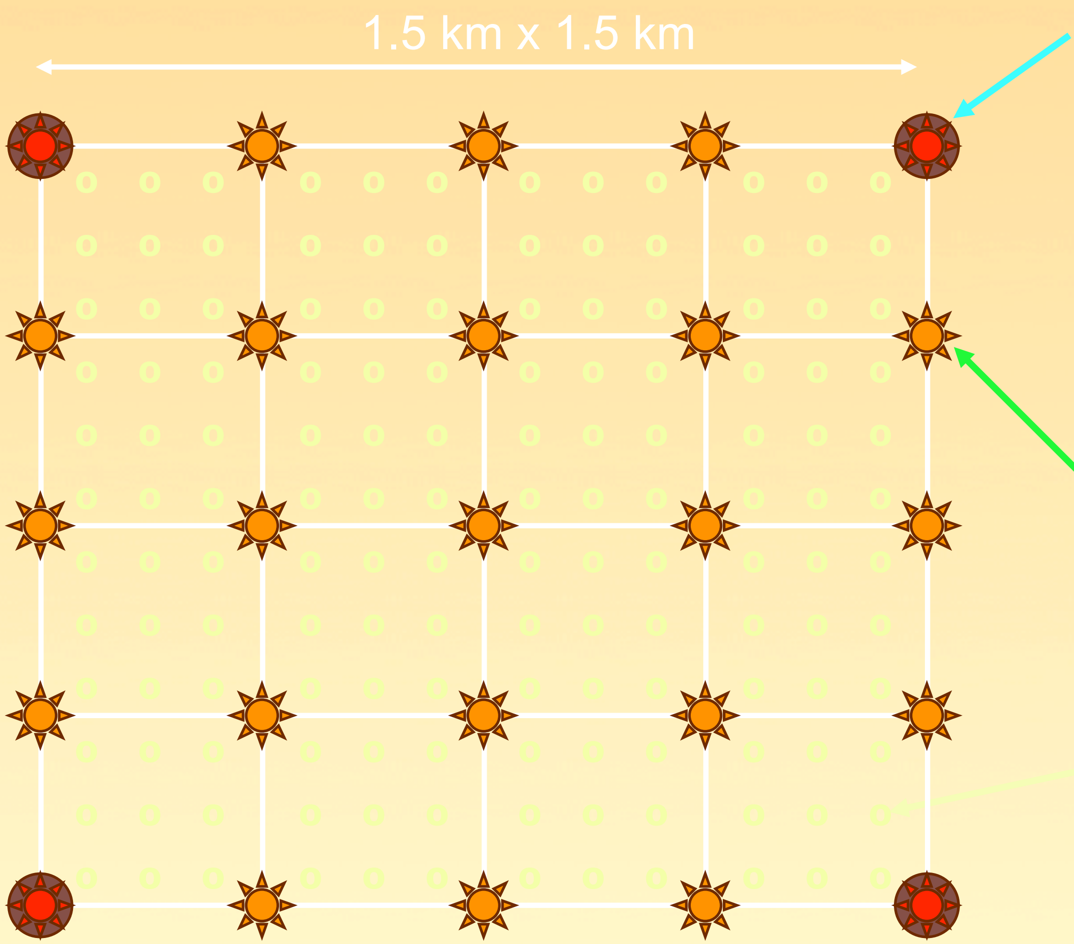

Source parameters:

- Slip amplitude (A)
- Slip rake
- Rupture velocity
- Rise time (T)

Green's Functions (0.16 - 1.0 Hz)

Interpolated
- Source parameters
- Green's functions

Liu and Archuleta, JGR, 2004

Kinematics – forward modeling

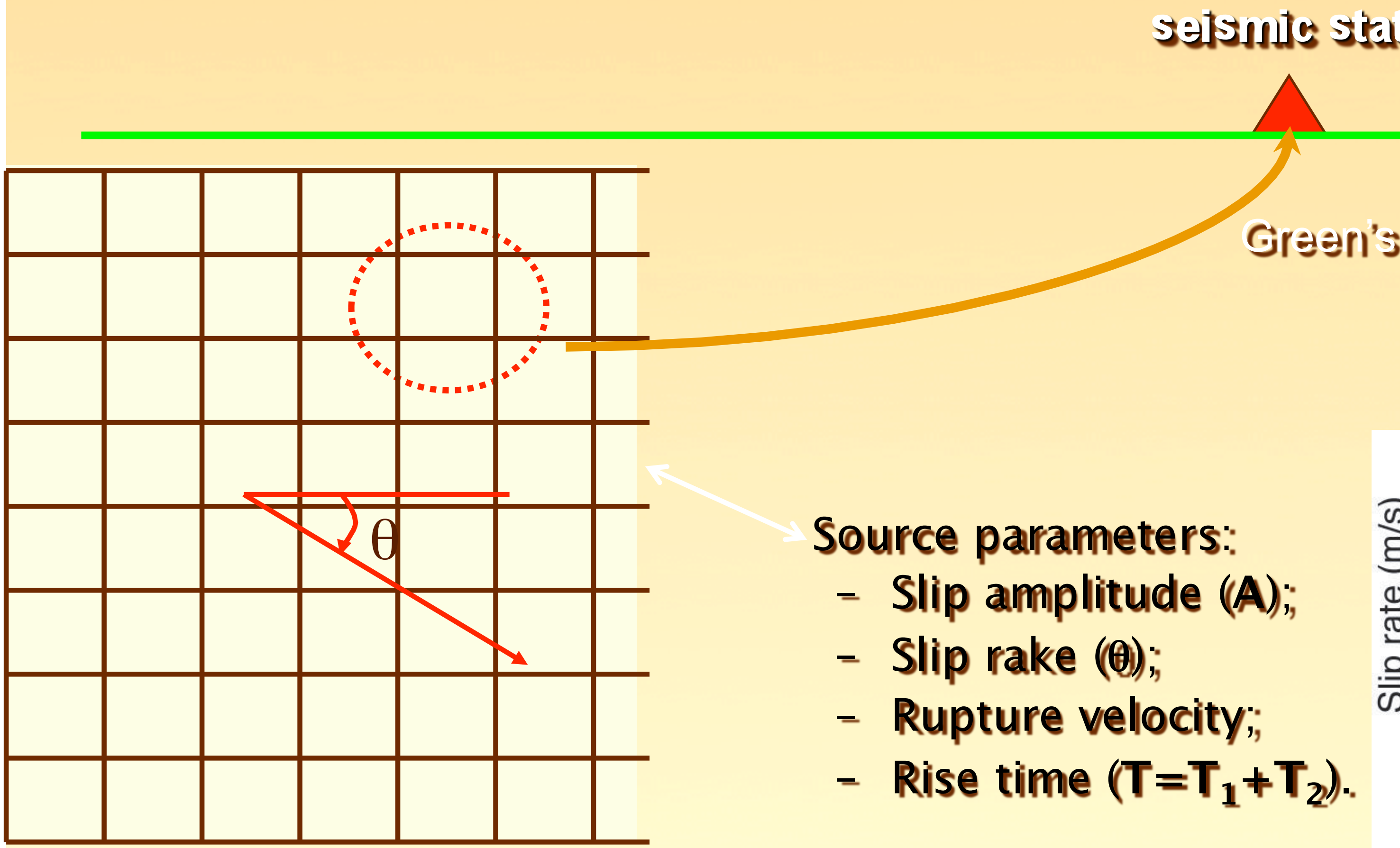

Source parameters:
- Slip amplitude (**A**);
- Slip rake (θ);
- Rupture velocity;
- Rise time (**$T=T_1+T_2$**).

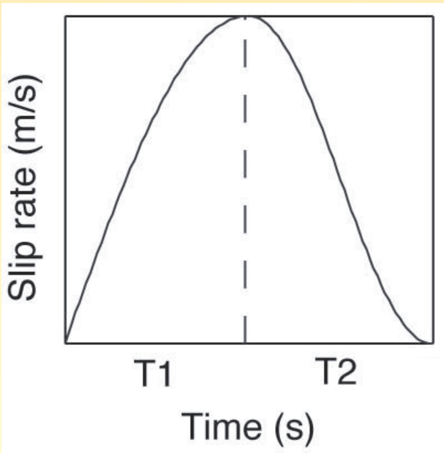

Isochrone Velocity

Isochrone velocity is directivity and is defined by

where

x is the observer location

y is a location on the fault

$t(\mathbf{y},\mathbf{x})$ is the arrival time at **x** of an S wave radiated from **y**

is the vector surface gradient of the arrival time

Arrival time t is defined as the sum of the rupture time t_r and the S-wave travel time t_s:

$$t(\mathbf{y},\mathbf{x}) = t_r(\mathbf{y}) + t_S(\mathbf{y},\mathbf{x})$$

Spudich and Frazer, BSSA, 1984

1999 Chi Chi Inversion

Accelergraphs and Geometry
Used to Invert for Rupture Parameters

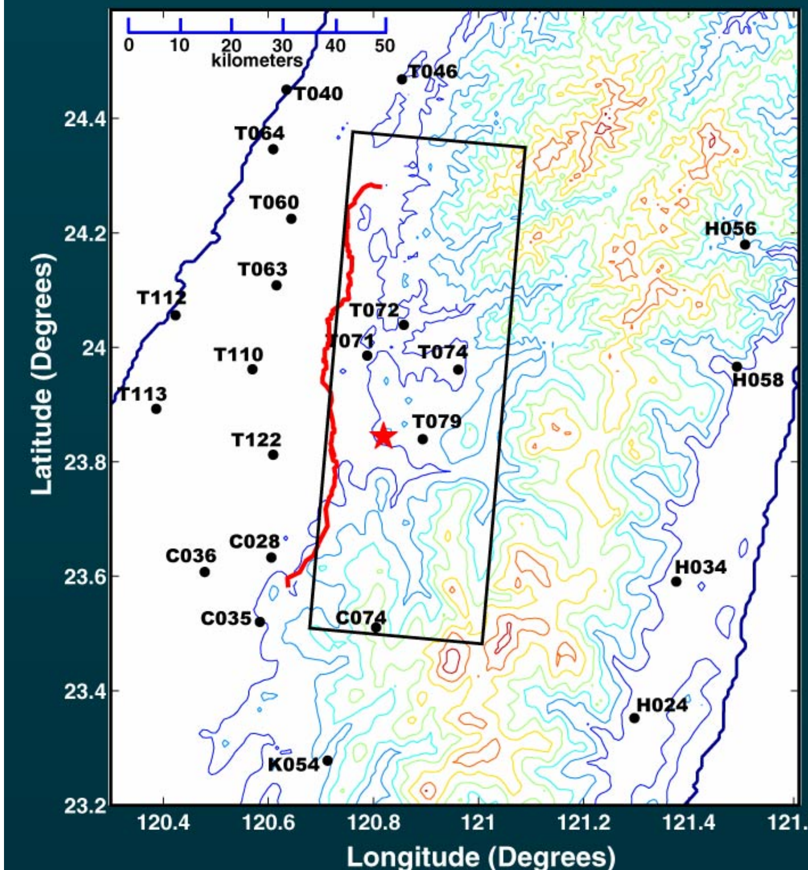

Velocity Structure

For 2 km and deeper we directly used the 3-D velocity of Taiwan area based on Chen, Teng, and Gung, JGR, 253-21,273, 1998)
At depths of 0.5 km, and 1.0 km we based the velocity structure on the model of Kuo Fung Ma (Chen Ji, personal communication).
We added Q model based on the Q model of Ma and Zeng.
$V_S min=0.9$ km/s, $V_P min=1.9$km/s
$Q_S min=50$, $Q_P min=100$
Grid is 150 km x 132 km x 32 km

Calculation of Green's Functions

We use the reciprocity of the Green's function and compute the tractions on the fault from 3 point forces at each station with a 4th order viscoelastic finite-difference (FD) method (Liu and Archuleta, 1999). Using a modified coarse grain method (Day, 1999) we model frequency independent Q. Second order absorbing boundary conditions are applied at all boundaries except the free surface.
Frequency band is 0.0 – 0.5 Hz. Grid spacing is 350 m.

Inversion of Data

A modified simulated annealing method based on the global inversion method of Liu et al. Using 22 stations (66 components) that provide 360° converage, the inversion has 6600 data to constrain 1170 parameters.

Parameters found by inversion: Slip Amplitude, Slip Rake, Rupture Velocity, Rise Time, Exponent "p" that controls the shape of slip rate function.

$$\dot{S}(t) = C\,(t/T)^p(1-t/T)^{5-p}$$

C: Normalization Constant
T: Rise Time

Liu and Archuleta, 2001

1999 Chi Chi Earthquake

Ground Motion Predicted from Fault Model

(Blue traces are data; red traces are predictions)

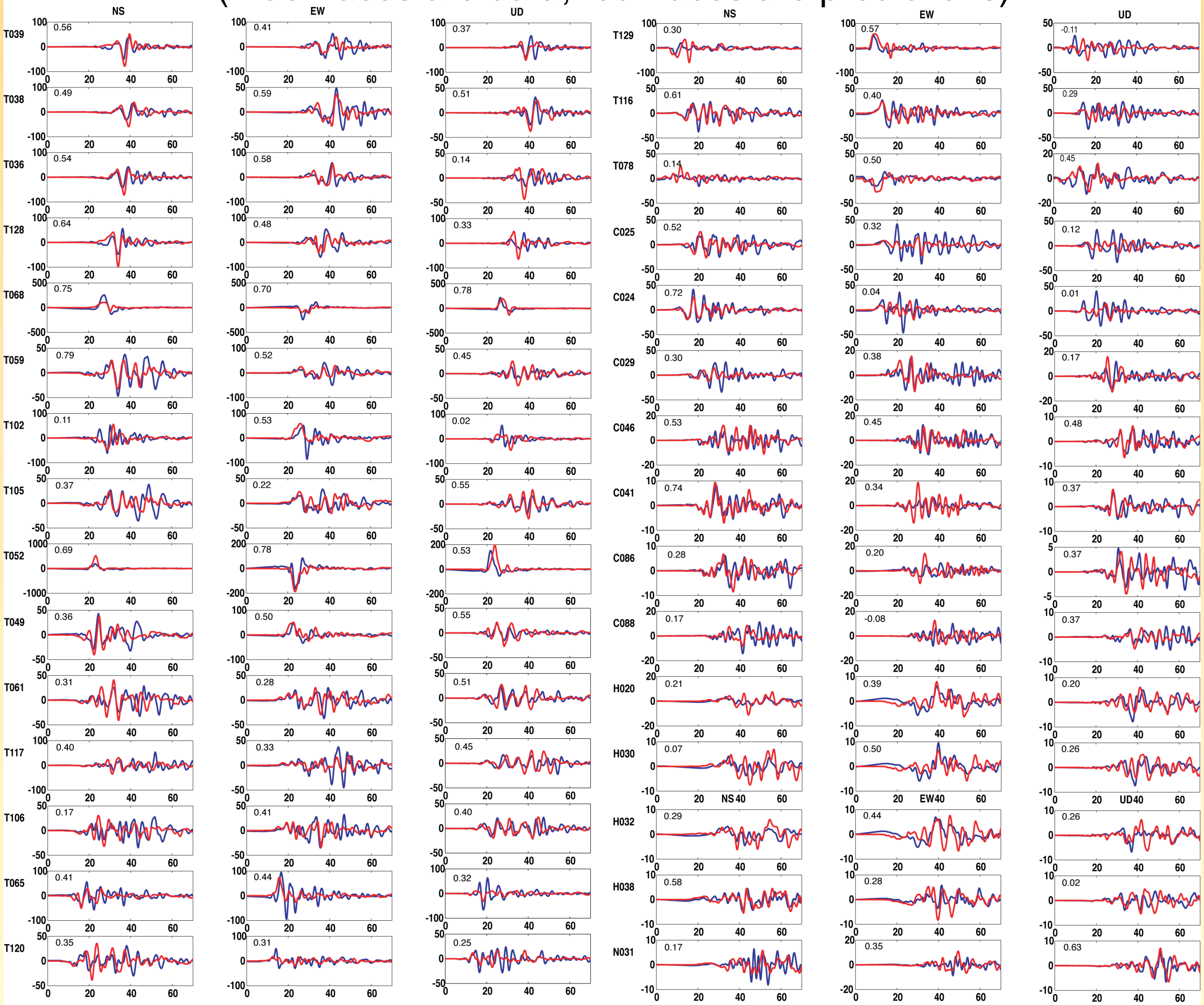

Liu and Archuleta, 2001

Grid Size

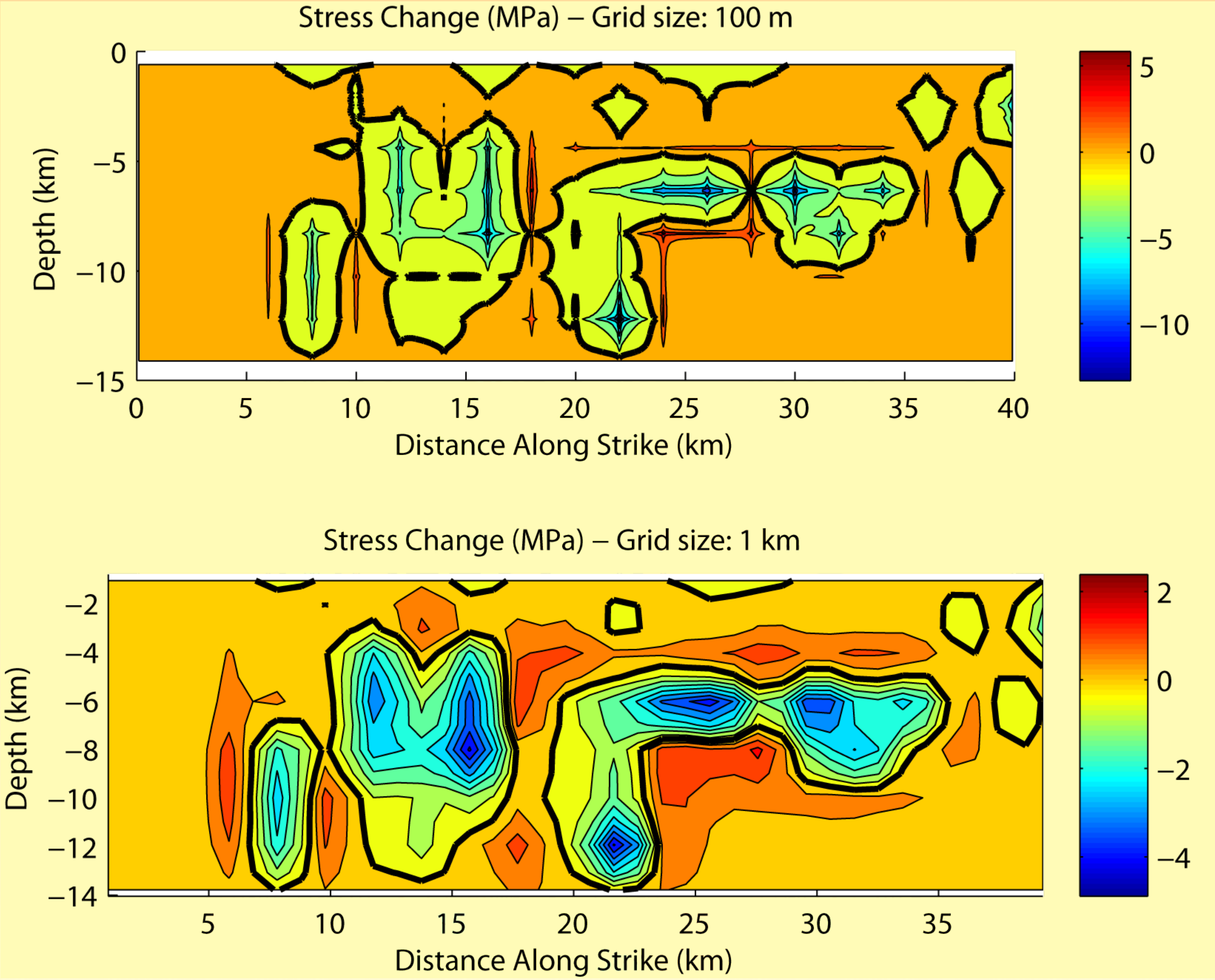

SCEC 2009 Annual Meeting Workshop

Ma (pers. comm., 2007)

Keiiti Aki
Seismic Displacements Near a Fault
(J. Geophys. Res., 1968)

$$U^l(Q,\omega) = D\Delta h\Delta l\left[A(\omega)\frac{\sin X_a}{X_a}\exp\left(-i\omega r/a - iX_a - i\omega l/v\right) + B(\omega)\frac{\sin X_b}{X_b}\exp\left(-i\omega r/b - iX_b - i\omega l/v\right)\right]$$

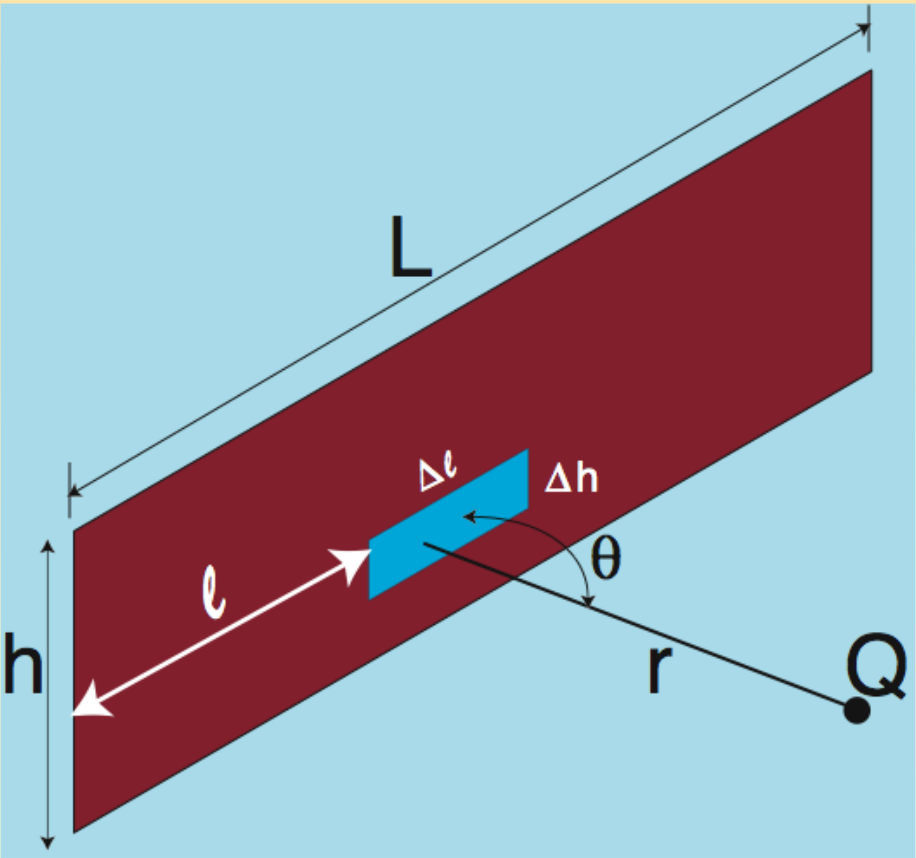

$$X_c = \omega\,(\Delta l/2)\left[(1/v) - (\cos\theta/c)\right]$$

$$D = D_0\frac{\left(h^2 - Z^2\right)^{1/2}}{h} \qquad 0 < Z < h$$

Total Motion at Q

$$U(Q,t) = FFT^{-1}\left[\sum_l U^l(Q,\omega)\right]$$